

Treball de Fi de Grau

**Grau en Tecnologies Industrials i Anàlisi
Econòmica**

**Design of the Fingers of a Soft-Rigid
Robotic Gripper Adaptable for Pinching
and Vacuum Grasping**

REPORT

Author: Guillem Tapia Palacio
Supervisor: Maria Alba Perez Gracia
Call: September 2023



Escola Tècnica Superior
d'Enginyeria Industrial de Barcelona



Resum

El projecte es centrarà en el disseny d'una pinça robòtica de dos dits que combini totes dues tecnologies de subjecció, la succió i el pinçament ("pinching"), per a convertir-se en un robot versàtil capaç de treballar amb objectes de formes variades.

La pinça estarà equipada per a incloure succió al llarg dels dits. A més, els dits estaran dissenyats de manera que permetin col·locar les ventoses per a diferents tipus de subjecció i, com a pinçament, succió horitzontal i vertical, tant en superfícies planes com corbes.

En primer lloc, es realitza un estudi de mercat basat en les solucions existents i els objectes que es desitja agafar per a trobar les millors especificacions.

Posteriorment, s'aplica una primera aproximació matemàtica per a tractar de trobar una pinça que realitzi la trajectòria desitjada basada en un únic mecanisme de barres. De l'estudi, s'extreuen algunes conclusions i es decideix fer un canvi d'estratègia.

Finalment, es dissenya un prototip basat en mecanismes independents i es dimensiona mitjançant un mètode gràfic. Es mostren els seus resultats, es crea un prototip en 3D i es presenten les conclusions.

Resumen

El proyecto se centrará en el diseño de una pinza robótica de dos dedos que combine ambas tecnologías de agarre, succión y pinzamiento, para convertirse en un robot versátil capaz de trabajar con objetos de formas variadas.

La pinza estará equipada para incluir succión a lo largo de los dedos. Además, los dedos estarán diseñados de forma que permitan colocar las ventosas para distintos tipos de agarre, como pellizcos, succión horizontal y vertical, tanto en superficies planas como curvas.

En primer lugar, se realiza un estudio de mercado basado en las soluciones existentes y los objetos que se desea agarrar para encontrar las mejores especificaciones.

Posteriormente, se aplica una primera aproximación matemática para tratar de encontrar una pinza capaz de realizar la trayectoria deseada basada en un solo mecanismo de barras. Del estudio, se extraen algunas conclusiones y se decide hacer un cambio de estrategia.

Por último, se diseña un prototipo basado en mecanismos independientes y se dimensiona mediante un método gráfico. Se muestran sus resultados, se crea un prototipo en 3D y se presentan las conclusiones.

Abstract

The project will focus on the design of a two-finger robotic gripper that combines both technologies of grasping suction and pinching to become a versatile robot capable of working with varied shape objects.

The gripper will be equipped for including suction along the fingers. Also, the fingers will be engineered such that they allow the positioning of the suctioning cups for different types of grasping, including pinching, horizontal and vertical suction, for flat as well as curved surfaces.

Firstly, a market study based on existing solutions and desired objects to grasp are done to find the best specifications.

Later, a first mathematical approach is applied to try to find a one linkage mechanism that performs the wanted trajectory. From the study, some conclusions are drawn and a change of strategy is decided.

Finally, a prototype based on independent mechanisms is designed and dimensioned by a graphical method. Their results are shown, a 3D prototype is created and conclusions are presented.

Contents

Resum	3
Resumen	4
Abstract	5
Contents	7
List of figures	8
List of tables	12
1. Introduction	14
1.1. Motivation	14
1.2. Objectives of the Project	14
1.3. State of the Art and Literature Review	15
2. Product definition and specifications research	18
2.1. Activity Definition	18
2.2. Statistical Analysis	19
2.2.1. Pinching	19
2.2.2. Suction	22
2.3. Morphology chart	26
3. Kinematic Design	29
3.1. Task Specification	29
3.2. Mathematical definition of the trajectory	30
3.3. First Approach	34
3.3.1. Structural Synthesis	34
3.3.2. Dimensional Synthesis	39
3.4. Final Approach	51
3.4.1. Structural Synthesis	51
3.4.2. Dimensional Synthesis	60
3.4.3. 3D design	80
3.5. Results, discussion, and simulation	80
4. Economic, environmental and social assessment	85
5. Conclusions	86
6. References	87

List of figures

Figure 1. RG2 OnRobot gripper [3]	16
Figure 2. Octopus gripper by Festo [4].....	16
Figure 3. MAXXgrip from TGC [7] and the RightPick™ Gripper [8]	17
Figure 4. “A Gripper System for Robustly Picking Various Objects Placed Densely by Suction and Pinching” project [5]	17
Figure 5. Weight histogram and weight boxplot.....	20
Figure 6. Friction histogram and friction boxplot.....	21
Figure 7. Required pinching force histogram and required pinching force boxplot.....	21
Figure 8. Dimensions histogram and dimension boxplot	21
Figure 9. Suction cup design guidelines [19].....	22
Figure 10. Forces definition for each case (including the safety coefficient “S” [19].....	23
Figure 11. Histogram and boxplot of safety required vacuum force	24
Figure 12. Histogram and boxplot of required number of suction cups	25
Figure 13. Objective work range [3]	29
Figure 14. Illustration of the three configurations based on OnRobot RG2 gripper [3].	30
Figure 15. Gripper picture with the axes specified [3].....	31
Figure 16 Geometric definition of variables [3]	31
Figure 17. Trajectory matrices results	33
Figure 18. Ideal trajectory plot.....	34
Figure 19. Kinematic pairs table [21].....	35
Figure 20. RRSS mechanism [22].....	38
<i>Figure 21. [D] definition [21].....</i>	<i>39</i>
<i>Figure 22. RRSS sketch</i>	<i>40</i>
Figure 23. D-H parameters representation of our case [21].....	41

<i>Figure 24. D-H transformations [21]</i>	41
<i>Figure 25. D-H Matlab code</i>	42
<i>Figure 26. [R] defined by b parameters [23]</i>	42
<i>Figure 27. [B] definition [23]</i>	42
<i>Figure 28. Bvector function definition</i>	43
Figure 29. Randomized variables on Matlab code	46
<i>Figure 30. Translation vector comparison</i>	47
<i>Figure 31. Rotation matrix and vector b comparison</i>	47
<i>Figure 32. Collection of 10 final candidates plots</i>	49
<i>Figure 33. Ideal trajectory plot</i>	50
Figure 34. Schematic representation of left finger of the gripper	52
Figure 35. Worm drive [24].....	54
Figure 36. Finger structure on two different positions.....	55
Figure 37. Suction switching system scheme with variables defined.....	55
Figure 38. Kinematic pairs transmission scheme	56
Figure 39. 3D representation of the right finger from bottom plane.....	56
Figure 40. Structural sketch of the locking mechanism	57
Figure 41. Scheme of the motion transmission of the locking system	58
Figure 42. Picture of the mechanism on the final 3D design.....	58
Figure 43. Commercial mini push-type catch latch.....	59
Figure 44. Picture of the mechanism on the final 3D design.....	59
Figure 45. Pictures of the first and last positions of the complete mechanism on the final 3D design	60
Figure 46. Structural schemes of the pinching system with dimension variables.....	60
Figure 47. One finger assembly of L1, L2, L3, L4.....	63

Figure 48. L1 industrial drawing	63
Figure 49. L4 industrial drawing	64
Figure 50. L4 component.....	65
Figure 51. Rotative fingertip and suction cup cover.....	65
Figure 52. L4 and fingertip assembly	66
Figure 53. Fingertip wheel dimensions.....	66
Figure 54. Fingertip assembly constraint.....	67
Figure 55. Fingertip wheel industrial drawing	67
Figure 56. Fingertip wheel assembly dimensions.....	68
Figure 57. Assembly with the wheel	68
Figure 58. Industrial drawing of the L2S dimension.....	69
Figure 59. Position dimensions of L2S with respect to L2. Note that is L2S is totally fixed with respect to L2.....	70
Figure 60. industrial drawing of the L6 dimension	70
Figure 61. Position dimensions of L6 with respect to L3. Note that only the axis is fixed to L3 but no all the part	70
Figure 62. Final assembly representation	71
Figure 63. L6 attachment representation.....	71
Figure 64. 3D picture and industrial drawing of M1	72
Figure 65. 3D picture and industrial drawing of M2	73
Figure 66. M3 dimensions.....	73
Figure 67. M assembly constraint	74
Figure 68. M assembly collision detection.....	74
Figure 69. M assembly vertical and horizontal displacement.....	75
Figure 70. 3D conditions verification	76

Figure 71. Conditions verification	76
Figure 72. Wheel hole.....	77
Figure 73. Entire locking mechanism representation.....	77
Figure 74. Worm gear variables [26].....	78
Figure 75. 3D prototype	82
Figure 76. Moments where the angles presented are calculated (initial and final positions for suction switching)	83

List of tables

Table 1. Applications table	18
Table 2. Friction coefficient (CoF) for each surface type.....	20
Table 3. Limit features decided for the gripper.....	22
Table 4. Suction cup dimensions [20].....	23
Table 5. Suction parameters decided	26
Table 6. Morphology chart table	27
Table 7. D-H parameters of our case	41
Table 8. Final parameters summary	62
Table 9. Parameters of the result	83

1. Introduction

Nowadays, many companies are facing new needs due to the growing market demand and the constant technological evolution. Therefore, betting on robotics has become an efficient solution to solve problems in various fields.

In large industries, specific robots have been developed to perform repetitive and simple tasks that do not require versatility. Nevertheless, most of the companies have to perform different tasks and with different objects each time while having less investment capacity, space or possibility of acquiring a robot specific for each task.

Although robots capable of performing different tasks already exist, many of them are limited by the using of only one type of grasping technology. This limits their ability to work with varied and complex objects and perform different tasks.

To address this problem, this project proposes a unique versatile robot capable of grasping different objects with varied shape features through the combination of pinching and suction.

This will allow smaller companies to take advantage of the benefits of robotics and improve their efficiency and productivity without incurring large investment costs.

1.1. Motivation

As I approached the end of my degree, I asked myself more and more insistently what specialty within engineering I would like to dedicate myself to. One of the fields that attracted me the most was robotics applied to improving the quality of life of people with functional diversity. This inspiration led me to investigate further and I found out the applications of robotics not only in healthcare, but also in industry and many other fields.

What attracts me the most about this specialty beyond its possible impact on society in the near future, is its potential related to technological innovation, its ability to promote the convergence of different disciplines and to build teamwork. And even more, its potential to develop valuable skills in research, design, programming and of course, problem solving.

1.2. Objectives of the Project

The main objective of this project is the design of a unique versatile robot capable of grasping different objects with varied shape features.

Goals:

- Design of the mechanical system of the new gripper and their integration in one assembly.
- Specific design of a suction action opening and closing system for suction cups.

Specific objectives:

- Selection of the appropriate combination of grasping technologies and conceptual design of the gripper based on the research of previous experiments, products and on the own study results.
- Design of a switching system that changes pinching to suction configuration and vice versa without adding a motor.
- 3D development of the new gripper prototype.
- Draw conclusions and think about the next steps to do outside our scope.

1.3. State of the Art and Literature Review

There are several means of grasping an object by a gripper. [1] [2]

- Pinching

These types of grippers use the two or more fingers to apply force to the object. Straight fingers rely on friction force while grooved or rounded fingers use local perpendicular forces to transmit the required force to maintain the object in a secure grip during handling. This is an example of a typical hard grip because a lot of force is always applied to the object.

- Enclosing

The gripper uses flexible or rigid fingers with broad surfaces to enclose the object partially or completely. The vector sum of all normal force vectors of the surfaces in contact with the object yields the force transmission to the object. This is a soft grip because the only forces acting on the object in this situation are gravity and the acceleration forces from the gripper walls.

- Pinning, penetration

The gripper has a number of pointed, sharp pins that are pressed into the object to form a locking pattern. This type of "grippers" are used for less rigid or pierceable objects such as cloth or food.

- Underpressure, suction

These grippers (often called “vacuum grippers”) create an underpressure in the gripping area with respect to the surrounding air. The pressure difference creates a force that pushes the object up against the gripping area. Release is obtained normally by removing the suction or occasionally by a slight overpressure.

Now let us perform a state-of-the-art study of the actual solutions on the market.

One of the most common and competitive grippers on the market is the RG2 Robot by OnRobot. It is a pinching 2-finger robotic flexible gripper with large stroke widely use on the industry. This will serve us a helpful reference for some of the structural and dimensional synthesis parts.



Figure 1. RG2 OnRobot gripper [3]

Also, there are several similar versatile robots on the market, to highlight the Octopus by Festo [4] and the Switchable central cap and two-finger gripper [5].



Figure 2. Octopus gripper by Festo [4]

But the aim of our project is to find a gripper that combines both the pinching and the suction to grasp the objects. Let us take a look now to the existing solutions on this field.

There are some grippers that use a combination of systems to maneuver with various objects or achieve various functionalities. It is the versatility what allows the grippers to provide new solutions to previously unsolved difficulties. The combination of pinching and suction system it is one of the best candidates to provide a reliable and versatile solution and it will be the one used. [6]

These most recent models are extremely novel and have yet to be commercialized. There are some recent models available, such as the MAXXgrip from TGC [7] or the RightPick™ Gripper from RightHand Robotics [8]. They combine both technologies to first grasp the objects by suction and then catch them by pinching to maintain them in a secure grip during handling.



Figure 3. MAXXgrip from TGC [7] and the RightPick™ Gripper [8]

Also, a new product called A Gripper System for Robustly Picking Various Objects Placed Densely by Suction and Pinching was presented in the IROS in 2018. This prototype combines both technologies but now having two different operating modes and a switch system. The first for using only the grasping by suction and the second for gripping the object by both suction and pinching. [5]

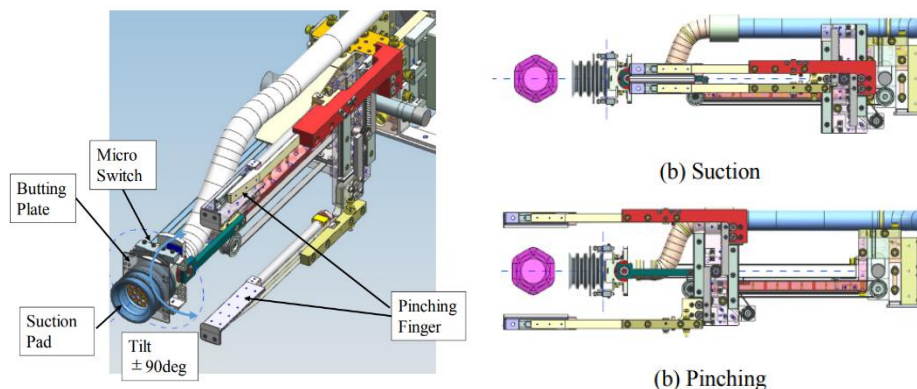
































Figure 4. “A Gripper System for Robustly Picking Various Objects Placed Densely by Suction and Pinching” project [5]

2. Product definition and specifications research

2.1. Activity Definition

The gripper is created for working in non-structural environments. At the present time, there are several sectors that could be interested in the technology: supermarkets, hospitals, pharmacies, laboratories, agriculture, home assistance and food delivering. A recompilation of applications for each sector is shown below with the aim of comparing them and selecting the final target of the gripper.

Table 1. Applications table

Sector	Index	1	2	3	4	5	6	7	8	9	10
Fresh Food Store											
Supermarkets and Minimarkets											
Hospitals and Medics											
Pharmacy, drugstores and cosmetics											
Home Assistance											
Food Delivering											

The sectors of fresh food, supermarkets and minimarkets, pharmacies, drugstores and cosmetics, clinic laboratory, home assistance and food delivering are the sectors that seem to fit better with the target idea of the project.

The first feature they share are the similar dimensions, weight and materials of which they are constructed. The alike dimension and weight of the objects allow to design a unique gripper with a size, mechanic design and power that satisfy adequately the requirements. For the materials, all are rigid or semirigid and not highly porous materials.

Also, the versatile gripper is useful in non-structure environments where the variety of objects require a combination of technologies to handle with them. If not, companies will prefer to acquire a more specific gripper only with that grasping technique. As it can be seen, all these sectors have this potential diversity on their items.

Finally, the limited accuracy of the gripper must be considered. In general, it is inherent on the concept of the versatility. Moreover, in this case the possibility of having the suction cups on the surface of the fingers makes the grasping even less precise. The sectors share not to have really small items and not so complex and precise work.

Harvesting in agriculture has been discarded because of the complexity, delicacy and accuracy of the applications. Also, specific clinic laboratory environments are considered too homogenous and structured spaces with repetitive equal tasks where a specific gripper would fit better.

Also, hospitality and odontology have been ruled out because of the small dimensions of some objects and limited accuracy of the gripper, as well as the hygiene restrictions that would force to contemplate.

2.2. Statistical Analysis

In order to decide the requirements for the gripper a statistical analysis among this collection of objects has been performed. The Excel file with all the statistical analysis is available also on the link of the 3D design specificized on the section 3D design.

2.2.1. Pinching

For the pinching, these are the main factors that will determine the requirements and the features of the gripper: the weight, the friction coefficient, the required normal force, and the dimension of external diameter of the suction cup. Although the weight and the friction coefficient are also considered as themselves, they are mainly used for calculating the required normal force that will determine the motor power. On the other hand, the pinching dimension will define the maximum achievable wide between the robot fingers.

The data on all the parameters mentioned of the objects presented has been collected. Research of the static coefficient of friction (COF) with different surfaces has been performed to use in the required force study. For the general cases, the mean values and clean and dry surfaces are considered. Exceptionally, if marked, the minimum value is considered as the coefficient on worst possible conditions related to the application: normally water or water and soap lubricated.

Table 2. Friction coefficient (CoF) for each surface type

SURFACE TYPE	FRICITION COEFFICIENT (COF) ¹
FRESH FOOD ² [9]	0.3
HDPE [10] [11]	0.6
PP, PET, PVC [12] [11]	0.2
CARDBOARD [13]	0.5
GLASS [14]	0.4
STAINLESS STEEL [15]	0.64
ALUMINUM [16]	0.51
RUBBER [13]	1.16
CERAMIC [17]	0.5
SUGAR CANE [18]	0.1

From the data, the following results are obtained.

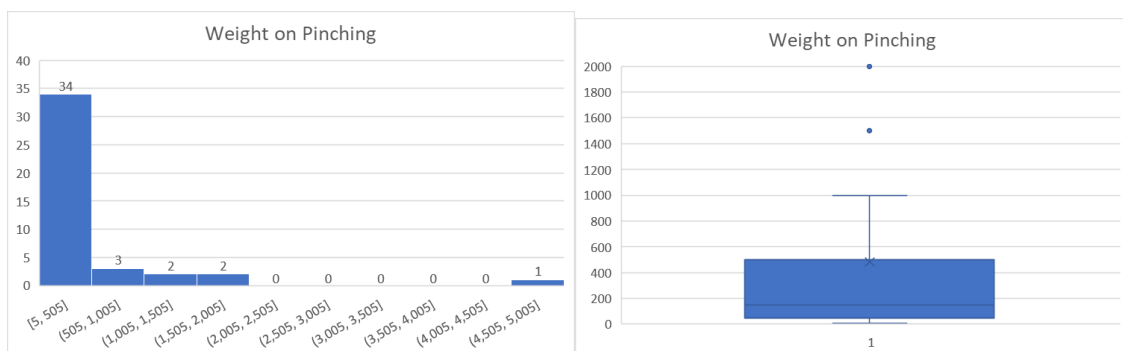


Figure 5. Weight histogram and weight boxplot

¹ Approximated values are taken as a reference for surface type.

² The food COF is approximated taken by the COF measured on tomato.

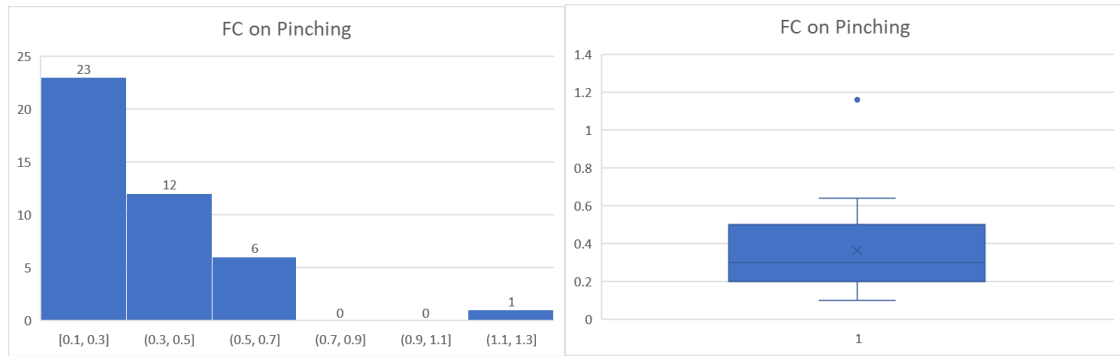


Figure 6. Friction histogram and friction boxplot

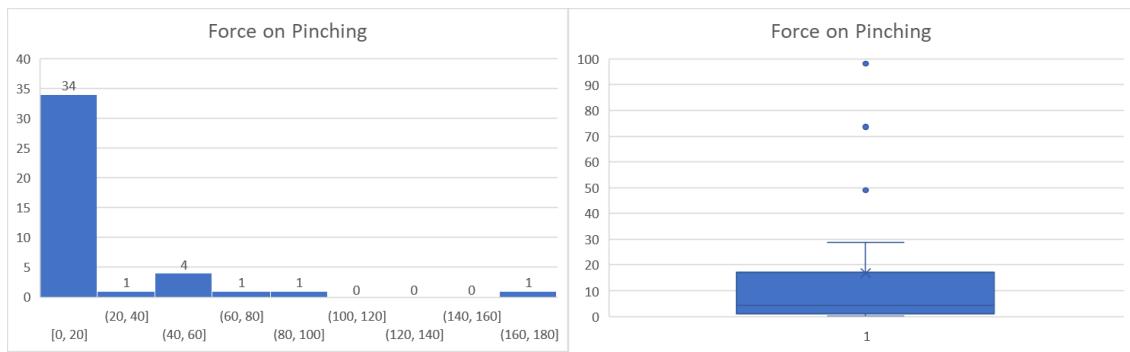


Figure 7. Required pinching force histogram and required pinching force boxplot

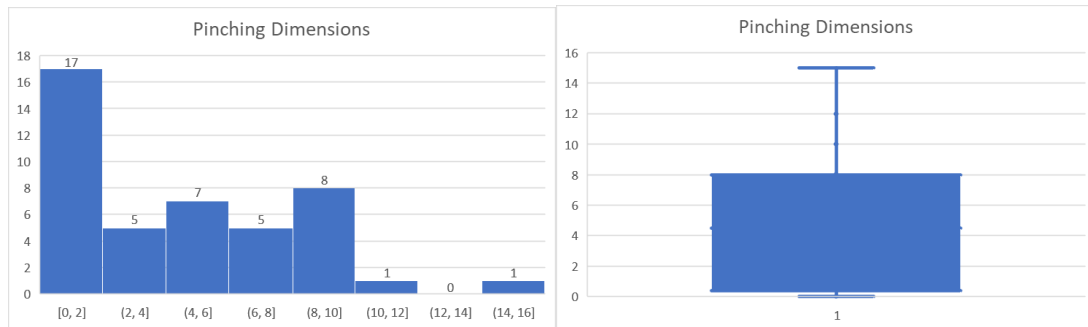


Figure 8. Dimensions histogram and dimension boxplot

The decision about the limits of the gripper’s features is the following. This also automatically defines the motor power and the operative wide range where the gripper can work.

Table 3. Limit features decided for the gripper

Feature	Minimum	Theoretical Maximum	Maximum without Safety Coefficient	Satisfied Percentile	Security Coefficient	Final Range
Weight (g)	0	2000	2240	97.73%	1.12	[0, 2000]
Normal Force (N)	0	98.1	110	97.73%	1.12	[0, 98.1]
Pinching Dimension (mm)	0	100	110	95.45%	1.1	[0, 100]

Also, note that the pinching dimension of 110 mm coincide with the common RG2 OnRobot gripper, something that corroborates somehow our approach.

2.2.2. Suction

For the suction cups, the overall design guidelines followed are captured in the table below.

Parameter	Effects on			
	Required suction force	No. of suction cups	Suction cup shape	Suction cup material
Workpiece dimensions	■	■	-	
Workpiece weight	■	■	■	
Workpiece rigidity	-	■	■	
Surface texture of the workpiece	Harsh	■	■	■
	Dry, wet	■	■	-
	Round, diagonal, curved	-	-	■
Environmental influences such as weather, cleaning agents, approval for use in the food industry, temperature	-	-	-	■
Distribution of suction grippers on the workpiece	■	■	-	
Arrangement of suction gripper in relation to direction of movement	■	■	■	
Max. acceleration	■	■	■	

Figure 9. Suction cup design guidelines [19]

The study is now split into the parameters to be selected: the Required Suction Force, the Number of Suction Cups, the Suction Cup Shape and the Suction Cup Material.


Suction Cup and Finger Dimensions

The first idea is to use relatively small suction cups as they should fit on the fingertip robot that is expected to be similar than the OnRobot RG2 gripper fingertip [20].

Besides, another considered is taken. For the efficiency of the suction system, all those cups that are not totally plugged in should be disconnected. Then, as the dimensions of the objects are different, the smaller the cups the more adaptability and efficiency of the suction on heterogenous objects. However, the stability is increased and the cost is reduced with bigger suction cups.

After taking all the reasons into account, it is selected as a reference the smallest option for the VG10 OnRobot prototype [20]. It has the following properties for each suction cup.

Table 4. Suction cup dimensions [20]

Image	External Diameter (mm)	Internal Diameter (mm)	Gripping Area (mm ²)
	15	6	29

Required Suction Force

The parameters studied are the following. It is been particularly important to consider an acceleration and the possible orientation of grasping like is shown below [19].

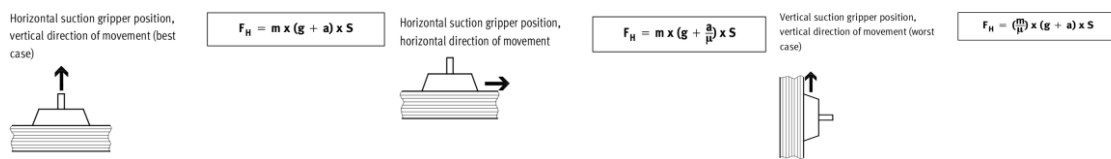


Figure 10. Forces definition for each case (including the safety coefficient “S” [19])

$$F_1 = m \cdot (g + a) \quad (\text{Eq. 1})$$

$$F_2 = m \cdot \left(g + \frac{a}{\mu} \right) \quad (\text{Eq. 2})$$

$$F_3 = \left(\frac{m}{\mu} \right) \cdot (g + a) \quad (\text{Eq. 3})$$

To extract information about the objects on the application table, these parameters are calculated for each of them.

- Weight of the object
- Friction coefficient: taken from Table 2.
- Acceleration: estimated on a maximum of $a = 10 \frac{m^2}{s}$
- Gravity: $g = 9.81 \frac{m^2}{s}$
- Maximum Required Vacuum Force (F). As shown in Figure 10, the required force is different depending on the orientation. The three are computed by the following equations presented before and the maximum is taken.
- Safety Required Vacuum Force (F_{safety}): $F \cdot 1.5$

And the results for all the objects on application table are the following.

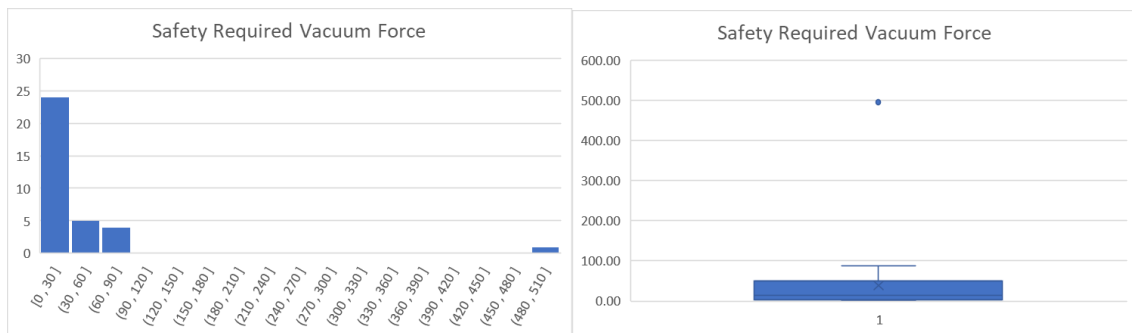


Figure 11. Histogram and boxplot of safety required vacuum force

Number of Suction Cups

The force will be applied by the suction motor that creates a difference of pressure. Let us characterize first this differential of pressure with a capacity of a motor of creating the 85% of vacuum.

$$P = 0.85 \cdot P_{atm} = 86126.25 \text{ Pa} \quad (\text{Eq. 4})$$

The parameters studied are the following:

- Effective Area per Cup ($Area_{cup}$): in our case considered of 29 mm as shown in Table 4.
- Required Vacuum Area ($Area_{Req}$): $\frac{F_{safety}}{P}$

- Required Number of Cups (N_{cups}): $\frac{Area_{Req}}{Area_{cup}}$

And the results for all the objects on application table are the following.

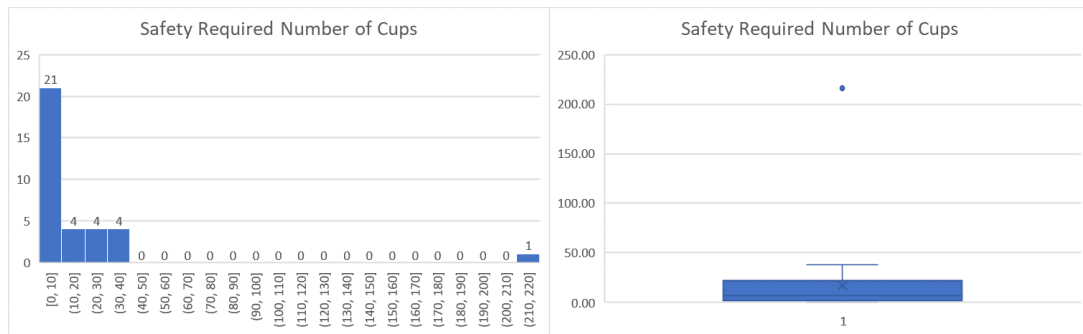


Figure 12. Histogram and boxplot of required number of suction cups

Suction Cup Shape

There exists different type of cups depending on the surface applications. The main are: the standard suction cups, the extra deep suction cups, the oval suction cups and the bellows.

It is necessary to have an adaptable suction cup because of the object's diversity. Then, let us study and select the best fit option.

The standard suction cups will be the first to be discarded, as are ideal for flat surfaces but have a lot of difficulties for all other type of surfaces. The oval suction cups are specifically designed for narrow and oblong workpieces such as profiles but have again a lot of problems with other types of surfaces. The extra deep suction cups are designed for exigent cases such as round or deeply undulation workpieces, something that provides good adaptability to the rest of cases. Finally, the most adaptable option: the bellows. As in previous cases, they fit with undulating, round and flat surfaces but the most interesting feature is that they can accommodate to inclined surfaces (from 5° to 30° depending upon suction cup diameter) and to flexible workpieces with large surfaces areas. It is also the best choice to work with fragile workpieces such as glass bottles.

Having exposed the arguments, the bellows are selected as the suction cup shape because of their adaptability.

Among the bellow cups are different possibilities regarding the number of fold or convulsions. More convulsions provide more adaptability to the gripper while could cause more problems with the moment forces and allowable mobility. As they will be the contact surfaces also when the pinching is performed and for a first design, it is decided to choose the minimum number of folds that represents the safer and most common option: the 1.5 convulsions. In future projects, if no problems are observed on the moment forces

on the cups when pinching is used, a more folded cup can be select to increase the adaptability.

Suction Cup Material

Silicone rubber is selected as the most appropriate material for suction cups. It is the most widely used, the only one approved for the food industry, it is suitable for low and high temperatures and resistance to water.

Final Selection

Taking into consideration all shown study of the application table objects the following decision is made. A first selection is made for an initial design with one finger per each finger allocated on the fingertip. For future improvements of the gripper, it is planned to study also other suction cups on the gripper links and not only on the fingertip. Thus, the number of suction cups could be considerably increased and their suction range improved.

Table 5. Suction parameters decided

Parameter	Suction Force	Percentage included	Suction Cup Shape	Cup Dimensions (Diameter)	Number of Suction Cups	Suction Cup Material
Gripper fingertip	4.59N	17.65%	Bellow 1.5 convulsions	15/6 mm	2 (1 per fingertip)	Silicone

2.3. Morphology chart

The morphological chart is a method to generate ideas in an analytical and systematic manner. It provides a structured approach to concept generation to widen the area of search for solutions to a defined design problem.

To do it, it is necessary to make on a table the flowing procedure. the first step is to list the product functions. Then, the possible means or solution for each function are listed. Finally, the last step is to chart functions and means and explore combinations. Therefore, a final conceptual solution is decided base on the morphology chart.

The next morphology chart is elaborated.

Table 6. Morphology chart table

Group	Function						
Pinching	Numbers of Fingers and Distribution	2: Parallel / Baseball Hand	3: in Parallel / 3 triangle / 3 <u>movable</u> (Barrett hand)	4: Four Together / 2x2 Actioned / 2+2 Parallel Actioned	5: Anthropomorphic 5 fingers	Finger(s) Retractable	
	For Small Objects 3D	Fine + Rigid Fingertips	Deformable fingertip	2 fingers always (not more)	Basket Finger		Magnet (for ferromagnetic materials)
	2D	Dragging or folding finger (high friction + compliant fingertip)	Soft fingertip	Dimples (if we can deform)	Fingernail (to lift object)		
	Position of Suction Cups	Central	Front of the fingers	Back of the fingers	Side Fingers	End Tips Fingers	Palm
Suction	Distribution along the Finger	Along the Finger	Along the Finger except on tip	Suction Tip	Mixed along the finger	Parallel Rows	Interleaved Rows
	Suction Pipes Distribution	No pipes (manifold)	Lateral Pipes	Vertical Pipes	Main tube with branches	Articulated/ball joint for cups	
	For Small Objects 3D	Small Cup(s) on End Tips Fingers	Suction (Inclined) Basket Finger	Pressurized Air Expulsion + Basket Finger	Combination of Pressurized+ Suction Basket Finger	Suction + Folding Mini Fingers	
	2D Flexible Objects (f. e. film)	Flat Inlet Mesh/Filter	Suction + Closing Baseball Finger				
	Grasping Movement of Fingers and Orientation of Cups	Fingers horizontal and inclined opening	Passive orientation of cups				
	Orientation of Cups	Active Orientation of Cup face	Passive Orientation of Cup face				
	Impurities	No filter	External Removable Filter Discs	External Fixed Filters	Internal Removable Filter Discs	Internal Fixed Filter	
Tasks	Pinching-Suction Position Switch	No switch: Pinching with cups on same face	Orientation switch: Pinching and cups on different fixed faces	Face switch: Pinching and cups on different rotary faces			
	Orientation	Vertical Rotation	Inclination				
	Peel	Actioned forceps in the tip end	2 grippers	Suction and Natural Separation	Suction and Horizontal Separation	Suction and Rotary Separation	

From all the possible combinations, this project will focus on the option “Cups on the internal face + parallel pinching + rotatory fingertip on the end of the trajectory”. Besides, the position of the suction plane forms a plane with low height in order that allows the gripper to adapt to the environment and entry into confined spaces. However, it is challenging option as the system of the turning faces plus the parallel movement requires a complex linkage system. Here it is a summary of the chosen ideal option for the final detailed design.

-
- Pinching: 2 parallel fingers with fingertips and parallel pinching movement.
 - Suction: 1 suction cup is located on the front of each fingertip, 2 in total.
 - Tasks: a parallel grasping movement for pinching and converted into a rotation to achieve a horizontal opened fingers for suction position, with 1 motor and through complex linkages or through independent mechanisms.

3. Kinematic Design

3.1. Task Specification

Based on previous sections, now it is the time to define specific conditions that will mark very strongly the final design. These are given by the needs of the market according to the study performed. The essential requirements for the new gripper are as follows.

Work Range

The pinching dimension objective is 110mm. As mentioned previously, it coincides with the one of the RG2 OnRobot model.

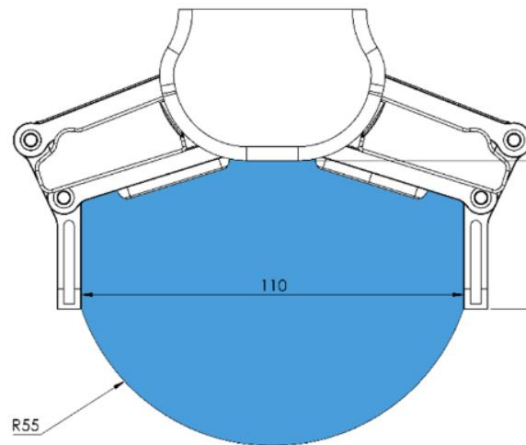


Figure 13. Objective work range [3]

Grasping configurations

The study is regarded on the trajectory of the front face of each finger. Its trajectory must have the following regions.

- I. Pinching grasping configuration: parallel aperture and closure of the fingers for pinching grasping with the fingertips looking at each other. This configuration is referred as pinching configuration, but there is also suction combined on the pinching as the option of a suction cup fingertip is selected.
- II. Switching movement to suction position: from the most opened position, a movement of the finger that turns 90° each face both to the floor but in opposite turning directions. This will be the most difficult part. The objective will be to find a mechanism that do it keeping only one already motor.
- III. Suction grasping configuration: the most parallel possible aperture closure and aperture with each finger pointing to the floor and kept locked on this 90° turned

position. Both finger faces form a rectangular planar plane formed by both faces, pointing to the floor and composed of the suction cups available for suction grasping. The more trajectory aperture the gripper is sable to do with the suction cups locked on suction position, the better the design. Ideally, the user can choose the angle of aperture of the gripper from any of the angles of aperture, like in the pinching configuration.

Therefore, it can be said the aim is to create a gripper that is able to work either in pinching or suction grasping configuration and also can make the change between configuration with the same motor.

Note that to apply the robot gripper frontally for the suction configuration, a 90° turn from the pinching configuration of the entire gripper unit would have to be performed to take the same object, something that will be assumed from now on to be performed by the mechanical arm.

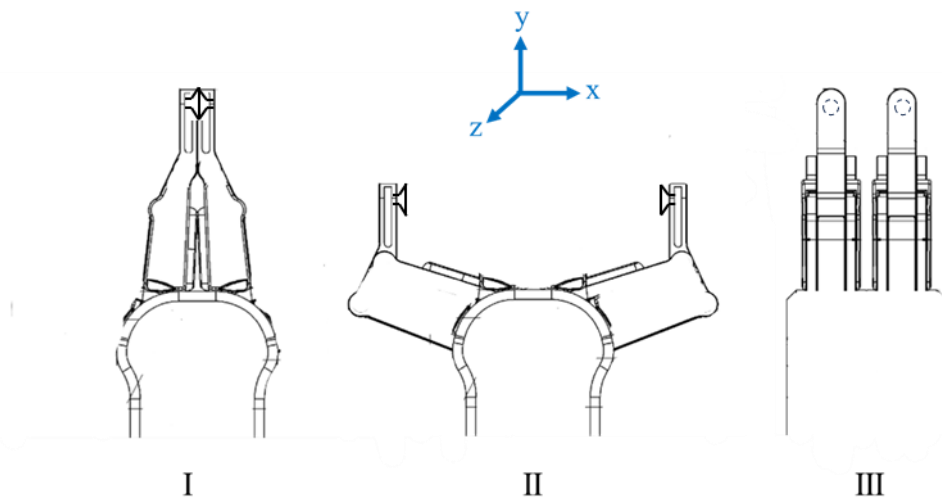


Figure 14. Illustration of the three configurations based on OnRobot RG2 gripper [3]

3.2. Mathematical definition of the trajectory

For the trajectory definition, it is important to define both the position and the orientation. In this case, the studied point (Point F) will be the end of the fingertip belonging to the front face and centered in its width. And the orientation (Orientation F) will be the one of the front face of the finger. The points and the axes are clarified in the following figure. This fixed reference frame is conserved on all the study of the project.

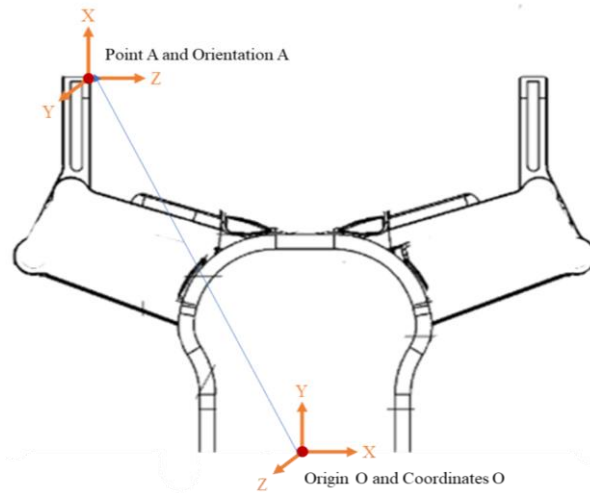


Figure 15. Gripper picture with the axes specified [3]

This trajectory is generated in order to create a reference where the trajectory of the mechanism created should fit to. For the mathematical definition, it is taken 11 points to define all the trajectory. The study is based on the geometry and the variables are specified on this figure. All the distances are referenced on three point: the origin (O), the circle of the circle of trajectory (Co) and the tip of the fingertip (A).

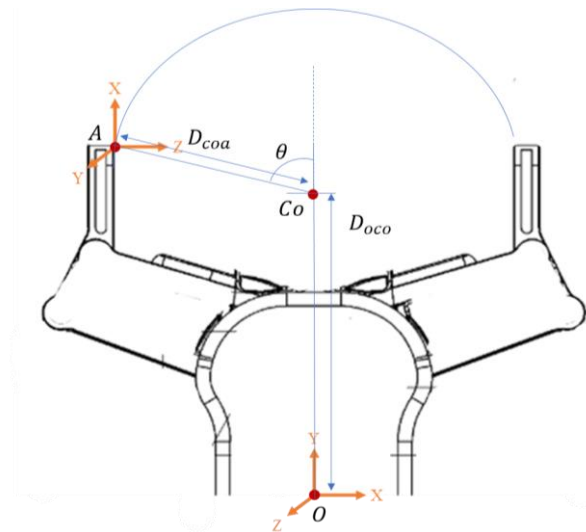


Figure 16 Geometric definition of variables [3]

The following variables are defined.

$$D_{coa} = R_{trajectory} = 110 \text{ mm} \quad (\text{Eq. 5})$$

$$D_{oco} = 26 \text{ mm} \quad (\text{Eq. 6})$$

A geometrical study is done to find the expressions for the position and orientation matrices. When had the expressions, a computation of all the positions and orientations is performed with Matlab software and derived from a geometrical study based on Figure 16. Please see the entire code ("trajectory.m") on the appendix documentation.

For the positions, the following equations are used to create the three items of the position vector and orientation vector and matrices. Let us note d as the translation vector that defines the position of the fingertip and $[R]$ as the rotation matrix that defines the orientation of the local reference frame of the fingertip, in accordance with the explained on Section 3.3.2.1. . Let us present then the equations imposed on each part of the trajectory.

On the parallel pinching congfiguration, from $\theta = 0^\circ$ to $\theta = 72.4^\circ$ in steps of 15° :

$$\theta = 0^\circ, \theta = 15^\circ, \theta = 30^\circ, \theta = 45^\circ, \theta = 60^\circ, \theta = 72.4^\circ \quad (\text{Eq. 7})$$

$$d = [d_x, d_y, d_z] = [0, -D_{coa} * \sin(\theta), D_{oco} + D_{coa} * \cos(\theta)]$$

$$[R] = \begin{bmatrix} 0 & 1 & 0 \\ 0 & 0 & 1 \\ 1 & 0 & 0 \end{bmatrix}$$

On a switching intermediate position, for $\theta = 60^\circ$:

$$\theta = 60^\circ$$

$$d = [-15, -D_{coa} * \sin(\theta), D_{oco} + D_{coa} * \cos(\theta)]$$

$$[R] = \begin{bmatrix} 0 & \cos(45^\circ) & -\sin(45^\circ) \\ 0 & \sin(45^\circ) & \cos(45^\circ) \\ 1 & 0 & 0 \end{bmatrix}$$

On the horizontal suction configuration, from $\theta = 45^\circ$ to $\theta = 0^\circ$ in steps of 15° :

$$\theta = 45^\circ, \theta = 30^\circ, \theta = 15^\circ, \theta = 0^\circ$$

$$d = [-30, -D_{coa} * \sin(\theta), D_{oco} + D_{coa} * \cos(\theta)]$$

$$[R] = \begin{bmatrix} 0 & 0 & -1 \\ 0 & 1 & 0 \\ 1 & 0 & 0 \end{bmatrix}$$

Through this the code, the following matrices are obtained. Where each row of the positions (Ptotal matrix) and every three rows of the orientations (Ototal matrix) correspond to one of the 11 points defined.

Ptotal =			Ototal =		
0	0	81.0000	0	1.0000	0
0	-14.2350	79.1259	0	0	1.0000
0	-27.5000	73.6314	1.0000	0	0
0	-38.8909	64.8909	0	1.0000	0
0	-47.6314	53.5000	0	0	1.0000
0	-52.4351	42.6000	1.0000	0	0
0	-52.4351	42.6000	0	1.0000	0
-15.0000	-47.6314	53.5000	0	0	1.0000
-30.0000	-38.8909	64.8909	1.0000	0	0
-30.0000	-27.5000	73.6314	0	1.0000	0
-30.0000	-14.2350	79.1259	0	0	1.0000
-30.0000	0	81.0000	1.0000	0	0
			0	1.0000	0
			0	0	1.0000
			1.0000	0	0
			0	1.0000	0
			0	0	1.0000
			1.0000	0	0
			0	0.7071	-0.7071
			0	0.7071	0.7071
			1.0000	0	0
			0	0	-1.0000
			0	1.0000	0
			1.0000	0	0
			0	0	-1.0000
			0	1.0000	0
			1.0000	0	0
			0	0	-1.0000
			0	1.0000	0
			1.0000	0	0
			0	0	-1.0000
			0	1.0000	0
			1.0000	0	0

Figure 17. Trajectory matrices results

When all the eleven positions and orientations are defined, the trajectory is 3D plotted. They are the local fingertip axes defined in figure Figure 15 represented by the RGB equivalency.

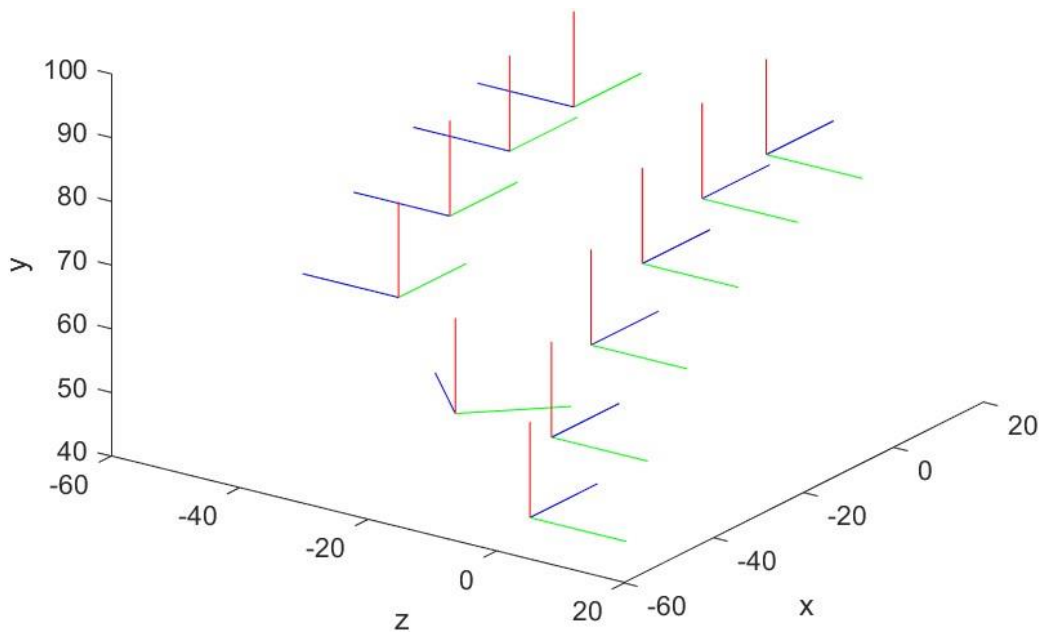


Figure 18. Ideal trajectory plot

3.3. First Approach

In this section, a first mathematical approach is applied to try to find a one mechanism system for the gripper. It is searching a one complex linkage system that satisfies the task specification defined. It should be noted that that the study is centered on just one finger, the left. For constructing the entire gripper, the finger should be replicated symmetrically.

The aim is to find a one complex linkage that can achieve all the task specifications. First, it should be able to perform a parallel pinching. And later, it must move to the suction configuration, and preferably conserving also the parallel orientation when the suction configuration is set.

Then, a complex linkage system is required in order to reach a 3D movement that change the orientation of the links at some point of its trajectory and keep it constant when it is necessary. It is a difficult challenge that is expected to require a complex system based on more than one type of kinematic pairs.

In the structural synthesis it is tried to select the best possible combination of links and joints. Once chosen one, a dimensional synthesis is performed to find the optimal dimensions for the linkage.

3.3.1. Structural Synthesis

In this chapter, first research will be done to find possible candidates of combinations of links and joints. Among all them, only one candidate is selected to continue the study.

The first step is to define the desired mechanism degree of freedom. As the gripper is expected to own only one motor and the movement of the linkage is wanted to be totally restricted by this unique active joint, the degree of freedom is set to 1.

As shown in the following picture, each type of kinematic pair restricts a particular motion and keeps free a specific number of degrees of freedom [21].



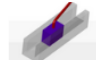







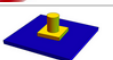
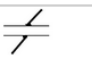




Name	Symbol	Example	Sketch	Allowed motion	Degrees of freedom f_i
Revolute or hinge joint	R		 entre barras con el suelo	Rotation about an axis	1
Prismatic or slider joint	P			Translation along a direction	1
Cylindrical joint	C			Rotation and translation about and along an axis	2
Spherical joint	S			Any rotation	3
Universal joint	U			Two rotations about perpendicular axes	2
Planar joint	E			Translations on a plane and rotations about a perpendicular axis	3
Pin-in-slot joint				Translations along a direction and rotations about a perpendicular axis	2
Cam joint				Sliding and pivoting on a point / line	2

Figure 19. Kinematic pairs table [21]

Now, it is needed to find possible combinations of joints and links that gives us a result a 1 DoF linkage. Then, a python base code owned by the Professor Alba Perez Gracia is used in order to create a list of those possible combinations. Let us present first the code.

3.3.1.1. Code Base

This code computes the possible combinations of solids and joints for achieving a selected degree of freedom.

First, some inputs with their initial values must be defined.

- M : selected degrees of freedom.
- n_{min} : minimum number of links, including ground.
- n_{max} : maximum number of links, including ground.
- p_{lo} : lower bounds on the number of joints (total).
- p_{up} : upper bounds on the number of joints (total).

- p_{u1} : upper bounds on the number of joints with one degree of freedom (R or P joint),
- p_{u2} : upper bounds on the number of joints with two degrees of freedom (C, pin-in-slot or cam joint)
- p_{u3} : upper bounds on the number of joints with three degrees of freedom.

Then, each p_{u1} , p_{u2} and p_{u3} represents a restriction on the total mechanism. By the iteration of a complex process defined on the appendix, only the combination of structure that satisfies the degree of freedom condition measured by the spatial Kutzbach-Gruebler formula are given as an output.

$$M = 6 \cdot (n - 1) - 5 \cdot p_{u1} - 4 \cdot p_{u2} - 3 \cdot p_{u3} \quad (\text{Eq. 8})$$

After executing a lot of iterations, the code gives as outputs the possible combinations of solids and links in the following list, where the magnitudes are the same than the described before.

$$\text{Output} = [M, n, p_{u1}, p_{u2}, p_{u3}] \quad (\text{Eq. 9})$$

Once understood the code, this it is been the process followed.

1. Introduction of data on the inputs of the code.
2. Analysis of the results.
 - a. Addition of restrictions on the code and start the loop again.
3. Selection of distribution and representation of the graph (joint representation).
4. Representation of the structure (linkage representation).
5. Acceptation or discard of the candidate regarding the available and desired trajectory.

3.3.1.2. Structural enumeration, inputs and limits

Let us present the inputs with the initial values considered. It should be noted that there are a lot of possible combinations so strong limitation on inputs are recommended to be done to obtain a reasonable number of option possible to analyze. To highlight, a strong limitation of links is imposed and a high number of p_{u1} joints is allowed to reach to an easier linkage.

$$M = 1, n_{min} = 4, n_{max} = 6, p_{lo} = 4, p_{up} = 15, p_{u1} = 10, p_{u2} = 4, p_{u3} = 6$$

Using general and nonspecific limits gives a very large number of possibilities so difficult to analyze. The, part of the problem solving will consist of analyzing the results and adding restriction until having an enough small number of possibilities feasible to be studied individually.

The final restriction applied are compiled hereunder:

- i. Symmetry (the number of links (n) must be pair). To understand the restriction, it is necessary to explain that the finger will be located on a solid between two joints. Therefore, the symmetry ensures that the simplest system is followed in the both sides. Then, if each system of linkages in the two sides allows the finger to follow the same trajectory, the simplest one can be chosen on both sides. Also, equalizing the connectivity (i.e. the degree of freedom from the base to the finger) on both sides. To impose it, the following command is introduced on the code.

$$mech3D[jl][1] \% 2 == 0$$

- ii. From the total of joints, one must be a revolute joint (R). The motor has a rotatory output that must be action the mechanism through a revolute joint. Again, the following command is added on the code. Also, it is been contemplated on the joint representation (graph).

$$p_{u1} > 1$$

- iii. The mentioned revolute joint must be connected to the first solid, the hand palm. This is because the easiest location to perform the transmission is inside the hand palm. This limit is contemplated on the joint representation (graph).
- iv. A maximum of two joints on the hand palm (solid 1). The hand palm represents a restriction for its size. It is marked as a limit a total of two joints for each finger for them to fit in the hand dimensions. To impose it, it is been contemplated on the link drawing but no on the code.

3.3.1.3. Results and final candidate

With the introduced variables, these are the results obtained. The bold ones are the first studied as have a higher number of revolute joints that makes easier the analyzing. In case any of the option satisfy the goals, the other will be considered. Also, candidates with 4 links are considered simpler so they will be studied first.

- **[1, 4, 1, 0, 4], candidate**
- **[1, 4, 1, 3, 0], candidate**

- **[1, 4, 2, 1, 1], candidate**
- **[1, 4, 2, 0, 2], candidate**
- [1, 6, 1, 3, 4]
- [1, 6, 2, 1, 5]
- [1, 6, 2, 4, 1]
- **[1, 6, 3, 2, 2], candidate**
- **[1, 6, 4, 0, 3], candidate**
- **[1, 6, 5, 1, 0], candidate**

Also, a one more candidate is added. It is a spatial revolute-revolute-spherical-spherical (RRSS) mechanism and is the most general and simple spatial four-bar mechanism with two revolute and two spherical joints. It is not given as output on the code because it does not fulfill the Kutzbach-Gruebler formula, but it does have only 1 DoF. This occurs because by the formula would give 2 DoF but one is restricted because the alienation of one axis of the spherical joints. Then, resulting to a 1 DoF system and a possible candidate.

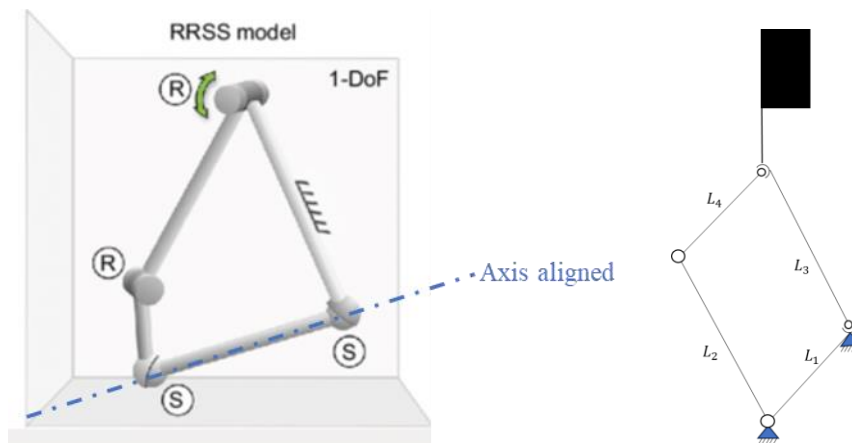


Figure 20. RRSS mechanism [22]

To study them, for each option it is been drawn a joint representation through graph theory and a after a linkage representation to see the resulting trajectory of the mechanism and try to find the best option based on it.

After all the study, RRSS is been selected as the most appropriate candidate. It satisfies all the objectives and thanks to its particular feature is able to perform a remarkable range of trajectories. After the linkage representation it is been seen that the trajectory it does could match with the one defined in the task specification. Also, it has only 4 links and 2 revolute joints that makes even more attractive this option.

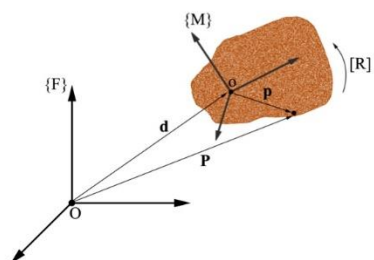
3.3.2. Dimensional Synthesis

Once having the structure, now it is the time for the dimensional. The aim is to find a combination of link dimensions and relative distances between their joints that gives a linkage that performs a trajectory similar to the task specification trajectory.

Mainly speaking, this is the process followed. Firstly, the trajectory followed by the fingertip is computed depending of all the dimensional variables through Denavit-Hartenberg method. Later, the objective trajectory is been mathematically defined. Through the code, a randomization of the variables obtained on the first step are randomized. Then, each case with different variables is compared on the position and orientation to the objective function in each of the eleven positions of reference. Finally, only those configurations where the sum of the differences along the eleven positions are less than a maximum tolerance set, are studied individually to find the best possible option. When all the possible candidates are collected, they are going to be analyzed if they are enough satisfactory. If they are, the closed loop equation will be imposed to find the best dimension and positions for spherical joints. This is because this last condition is expected to be so restrictive, by intuition and by some initial quick tests. Therefore, it is been decided first to perform a study of without this restriction, and only impose it to find the best selection for the resting variables if the results previously obtained are good enough.

3.3.2.1. Denavit Hartenberg study

The displacement matrix ($[D]$) is the matrix the displacement composites on a rotation matrix $[R]$ and a translation vector $[d]$. Then, specifies the position and orientation of the fingertip on the absolute axis. The collection of eleven $[D]$ matrices form the fingertip trajectory. It has the following form on its homogenous format.



$$[D] = \begin{bmatrix} & [R] & & \mathbf{d} \\ - & - & - & - \\ 0 & 0 & 0 & 1 \end{bmatrix}$$

Figure 21. $[D]$ definition [21]

Denavit-Hartenberg (D-H) method is used to find all the displacements matrices that conform the trajectory of the fingertip. In the study, they are calculated symbolically depending of all the dimensional variables of D-H method. As it is a closed loop system,

there are two paths. The path through the revolute joints is used to study the arrive to the fingertip point as it is the easiest (blue path on the figure). Then, with the calculated variables of the revolute joints the point of study is totally defined. However, after all the study, the results will be studied and the loop equation will be contemplated.

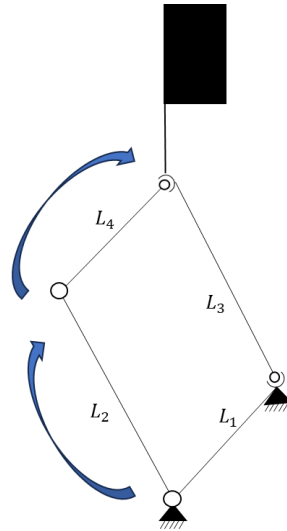


Figure 22. RRSS sketch

As mentioned, D-H method is matrix method that allows to systematically establish a coordinate system. The D-H representation establishes that by properly selecting the coordinate systems associated with each link, it will be possible to go from one to the next by means of 4 basic transformations that depend exclusively on the geometrical characteristics of the link.

The steps followed are the following:

1. Define joint axes S_i
2. Define common normal lines between axes A_{ij}
3. Align local z axis along joint axis, and local x axis along common normal lines
4. Four parameters suffice to move between the local coordinate frames

And the following representation and parameters of a 3D combination of 2 revolute joints are obtained. It should be noted that those parameter with asterisk are variable (free rotation axis of the revolute joint).

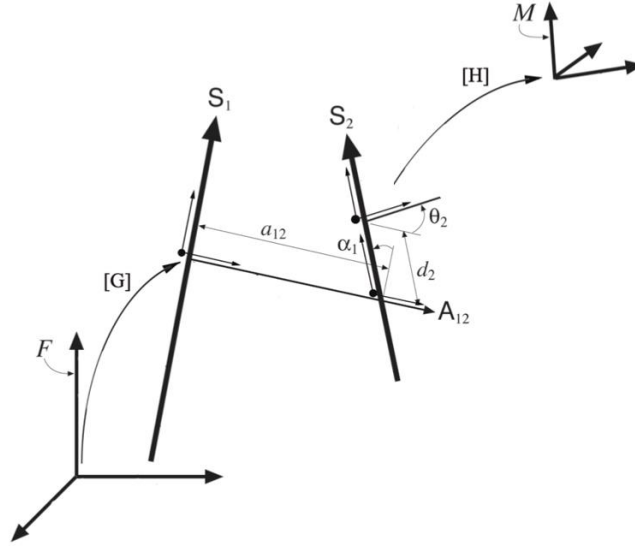


Figure 23. D-H parameters representation of our case [21]

Table 7. D-H parameters of our case

Local frame	$a_{i-1,i}$	$\alpha_{i-1,i}$	d_i	θ_i
1	a_{12}	α_{12}	d_1	θ_1^*
2	0	0	d_2	θ_2^*

From the parameters, transformations are applied using the following D-H formulas.

$$[D] = [G][X(\alpha_{01}, a_{01})][Z(\theta_1, d_1)][X(\alpha_{12}, a_{12})][Z(\theta_2, d_2)] \dots [X(\alpha_{n-1,n}, a_{n-1,n})][Z(\theta_n, d_n)][H].$$

$$[X(\alpha, a)] = \begin{bmatrix} 1 & 0 & 0 & a \\ 0 & \cos \alpha & -\sin \alpha & 0 \\ 0 & \sin \alpha & \cos \alpha & 0 \\ 0 & 0 & 0 & 1 \end{bmatrix} \quad [Y(\beta, b)] = \begin{bmatrix} \cos \beta & 0 & \sin \beta & 0 \\ 0 & 1 & 0 & b \\ -\sin \beta & 0 & \cos \beta & 0 \\ 0 & 0 & 0 & 1 \end{bmatrix}$$

$$[Z(\theta, t)] = \begin{bmatrix} \cos \theta & -\sin \theta & 0 & 0 \\ \sin \theta & \cos \theta & 0 & 0 \\ 0 & 0 & 1 & t \\ 0 & 0 & 0 & 1 \end{bmatrix}.$$

Figure 24. D-H transformations [21]

Resulting in our final matrix of displacement.

$$[D] = [G][Z(d_1, \theta_1)][X(a_{12}, \alpha_{12})][Z(d_2, \theta_2)][H] \quad (\text{Eq. 10})$$

Note that in Matlab code local variables are used to defined all this process and $[G] = [T_i]$ and $[H] = [T_f]$. Let us take a look on the code.

```

Xd=@(alpha,a) [1, 0, 0, a;
               0, cosd(alpha), -sind(alpha), 0;
               0, sind(alpha), cosd(alpha), 0;
               0, 0, 0, 1];
Zd=@(theta,t) [cosd(theta), -sind(theta), 0, 0;
              sind(theta), cosd(theta), 0, 0;
              0, 0, 1, t;
              0, 0, 0, 1];
Ti=[Rrand(b1i,b2i,b3i),drand(d1i,d2i,d3i);
    0,0,0,1];
Tf=[Rrand(b1f,b2f,b3f),drand(d1f,d2f,d3f);
    0,0,0,1];

Dsym=Ti*Zd(theta1sym,t1)*Xd(alpha1sym,a1)*Zd(theta2sym,t2)*Tf;

```

Figure 25. D-H Matlab code

3.3.2.2. Matrices study

At some point on the code, it will be necessary to compare two matrices. The rotation matrix that represents the orientation of the fingertip must be compared to the objective trajectory rotation matrix. The comparison of two matrices are not that easy, and for this reason a study is done.

In the reference “Kinematics of Robots” by Alba Pérez Gracia [23], a useful characterization of a matrix is explained. It is said that a rotation can be characterized by the rotation axis and rotation angle about the axis. Using Cayley's equation and Chasles' Theroem (also explained on the reference), it is possible to express the components of the rotation matrix as a function of the parameters of a vector $b = (b_1, b_2, b_3)$ that is related to the rotation axis and angle about the axis. It is obtained then the following expression [23].

$$[R] = [I - B]^{-1}[I + B] = \frac{1}{1 + b_1^2 + b_2^2 + b_3^2} \begin{bmatrix} 1 + b_1^2 - b_2^2 - b_3^2 & 2(b_1b_2 - b_3) & 2(b_1b_3 + b_2) \\ 2(b_1b_2 + b_3) & 1 - b_1^2 + b_2^2 - b_3^2 & 2(b_2b_3 - b_1) \\ 2(b_1b_3 - b_2) & 2(b_2b_3 + b_1) & 1 - b_1^2 - b_2^2 + b_3^2 \end{bmatrix}$$

Figure 26. $[R]$ defined by b parameters [23]

Where vector b is the assembly of the only three different elements of the matrix $[B]$ which is related to $[R]$ matrix.

$$[B] = \begin{bmatrix} 0 & -b_3 & b_2 \\ b_3 & 0 & -b_1 \\ -b_2 & b_1 & 0 \end{bmatrix}.$$

Figure 27. $[B]$ definition [23]

The interesting point is that now it is possible to compare two matrices by the comparison of only three values b_1 , b_2 and b_3 which are reliable and representative of the rotation matrix. But to do it, first it is necessary to extract the b vector from the $[R]$ matrices we are handling. Firstly, a transformation to the $[B]$ matrix format is needed. From the equations presented on Figure 26, the vector B is isolated from the $[R]$ rotation matrix.

$$[R] = [I - B]^{-1}[I + B] \quad (\text{Eq. 11})$$

$$[I - B][R] = [I + B]$$

$$[R] - [B][R] = [I] + [B]$$

$$[R] - [I] = [B][R + I]$$

$$[B] = [R - I][R + I]^{-1} \quad (\text{Eq. 12})$$

Then, the last equation is used to transform our rotation matrices $[R]$ to $[B]$. And the b vector is extracted from $[B]$ knowing the $[B]$ format explained on Figure 27. A function called “Bvector” is created on the code to streamline the process.

```
function Bvector = Bvector(O)
    OB=(O-eye(3))*inv(O+eye(3));
    Bfirst=OB(3,2);
    Bsecond=OB(1,3);
    Bthird=OB(2,1);
    Bvector=[Bfirst,Bsecond,Bthird];
end
```

Figure 28. Bvector function definition

Finally, each parameter of b vector between the objective and real matrices is compared. To quantify the difference, also a least squares method is used as will be explained on the creation of the code section.

4.3.1.1. Variables definition and creation of the code

Derived from the D-H process and matrices $[B]$ characterization, let us list the variables we will have. The objective of the dimensional synthesis then, it is become to find the feasible combination of these variables that crates a trajectory to most close to the objective. Also, let us present the limits imposed on these variables if they are created randomly. The limits are based on intuitive limits or on geometrical constraints of the gripper that can be seen on Picture 24.

From the homogenous transformation $[T_i]$,

- $b1i$: $[-50,50]$
- $b2i$: $[-50,50]$
- $b3i$: $[-50,50]$
- $d1i$: $[-30,30]$
- $d2i$: $[-20,-100]$
- $d3i$: $[-20,-60]$

From homogenous transformation $[T_f]$,

- $b1f$: $[-50,50]$
- $b2f$: $[-50,50]$
- $b3f$: $[-50,50]$
- $d1f$: $[-60,60]$
- $d2f$: $[-60,60]$
- $d3f$: $[-60,60]$

From D-H fixed parameters,

- $a1$: $[1,60]$
- $alpha1$: $[0,360]$
- $t1$: $[1,60]$
- $t2$: $[1,60]$

From D-H variable parameters along the 11 points of the trajectory. For this reason, they represent a total of 22 variables (2 per each of the 11 points) on the total trajectory.

- $theta1$: $[0, 360]$
- $theta2$: $[0, 360]$

Once explained the variables, let us centered on the code. Again, recall that the aim is to find the feasible combination of these variables that crates a trajectory to most close to the objective Also, it should be known that all the entire code is available on the appendix documentation (“eqsGT.m” and “FKequations2.m”), please take a look if necessary. The code follows the next steps:

1. Definition of objective trajectory
2. Randomly generation of some parameters
3. Construction of fingertip displacement matrix ($[D]$) by D-H method and symbolic resolution of resting parameters
4. Obtaining of the resting parameters by equation system solving of the equations generated on the objective trajectory
5. Construction of final $[D]$ matrix by D-H method with all the parameters
6. Comparison of the matrices by position and orientation and storage of the difference
7. Repetition of the code from step 3 only changing variables parameters are performed eleven times
8. Storage of the candidates where the sum of differences on the eleven loops is less than a tolerance number

And outside the code:

9. Analysis of the results and selection of final candidate

Let us explain all the process more accurately.

Definition of objective trajectory

The objective trajectory is the defined in the task specification section 3.2. .

Randomly generation of some parameters

The less the variables obtained randomly and the more obtained by equation system solving with the equations created by objective trajectory definition, the better for the code to speed up the finding of a good solution. However, because the complexity of the code, D-H process and especially the b vector matrix characterization, it is not been possible to use all the existing equations for the variable's determination. The parameters randomly generated by the Matlab function “randi” are the following.

```

% RANDOMIZATION
%D-H
a1=randi(60);
t1=randi(60);
t2=randi(60);

%Ti
b1i=randi(100)-50;
b2i=randi(100)-50;
b3i=randi(100)-50;
d1i=randi(60)-30;
d2i=randi(120)-20;
d3i=randi(80)-20;

%Tf
b1f=randi(100)-50;
b2f=randi(100)-50;
b3f=randi(100)-50;
d1f=randi(120)-60;
d2f=randi(120)-60;
d3f=randi(120)-60;

```

Figure 29. Randomized variables on Matlab code

Therefore, resting the following variables to be defined:

$$\alpha1, \theta1, \theta2, b1f, b2f, b3f$$

Construction of fingertip displacement matrix ([D]) by D-H method and symbolic resolution of resting parameters

The [D] displacement matrix of the tip of the fingertip is constructed by D-H method shown in Figure 25 but now solving it with all the resting variables list before handled as symbolical unknowns.

Determination of the resting parameters by equation system solving of the equations generated on the objective trajectory

The resting parameters are determined by system of equations solving of the equation generated on the objective trajectory.

On the first loop, the variables $\alpha1, \theta1, \theta2$ are determined by equalizing the translation vector (d) of calculated fingertip [D] to the one of the first point of the objective trajectory.

Also, the variables $b1f, b2f, b3f$ are determined by equalizing the b vector of the rotation matrix [R] of [D] to the first point b vector of [R] of the objective trajectory.

All the parameters determined on this section except $\theta1$ and $\theta2$ are keep constant along the 11 points of the trajectory. As already explained, the variable

parameters θ_1 and θ_2 are the only that vary along these 11 points. For this, the variables are not fixed and must be determined on each loop. To do it in the next loops, they are determined by equalizing the second (y-axis) and third (z-axis) items of translation vector (d) of calculated fingertip [D] to the analogous items of the ideal trajectory on the corresponding of the eleven points.

Construction of final [D] matrix by D-H method with all the parameters

Now, all the parameters are known on each loop. Then, the [D] matrix is constructed by D-H method.

Comparison of the matrices by position and orientation and storage of the difference

Now, there is a calculated [D] matrix and the ideal [D] matrix and both must be compared. For the translation comparison, the translation vector (d) is extracted from both matrix and the difference between them are computed using least squares method. The result is stored.

```
% POSITION COMPARISON
distPi=(x(i)-dinst(1))^2 + (y(i)-dinst(2))^2 + (z(i)-dinst(1))^2;
```

Figure 30. Translation vector comparison

In the same way, [R] matrix is extracted from both matrix. From both, the corresponding vector b is found by applying Bvector function explained on Figure 28. Again, the difference between each item is computed using least squares method.

```
% ORIENTATION COMPARISON
distBi=(b1(i)-Binst(1))^2 + (b2(i)-Binst(2))^2 + (b3(i)-Binst(1))^2;
```

Figure 31. Rotation matrix and vector b comparison

The result is stored and the difference is added on a total difference made up of the sum of the eleven differences.

Repetition of the code from step 3 only changing variables parameters are performed eleven times

All the parameters and differences are stored. And the loop is repeated from the step 3 until reaching 11 loops equivalent to the 11 points defined on the ideal trajectory. As explained, all the parameters remain fixed unless the variables ones (θ_1 and θ_2) that are redetermined in each loop.

Storage of the candidates where the sum of differences on the eleven loops is less than a tolerance number

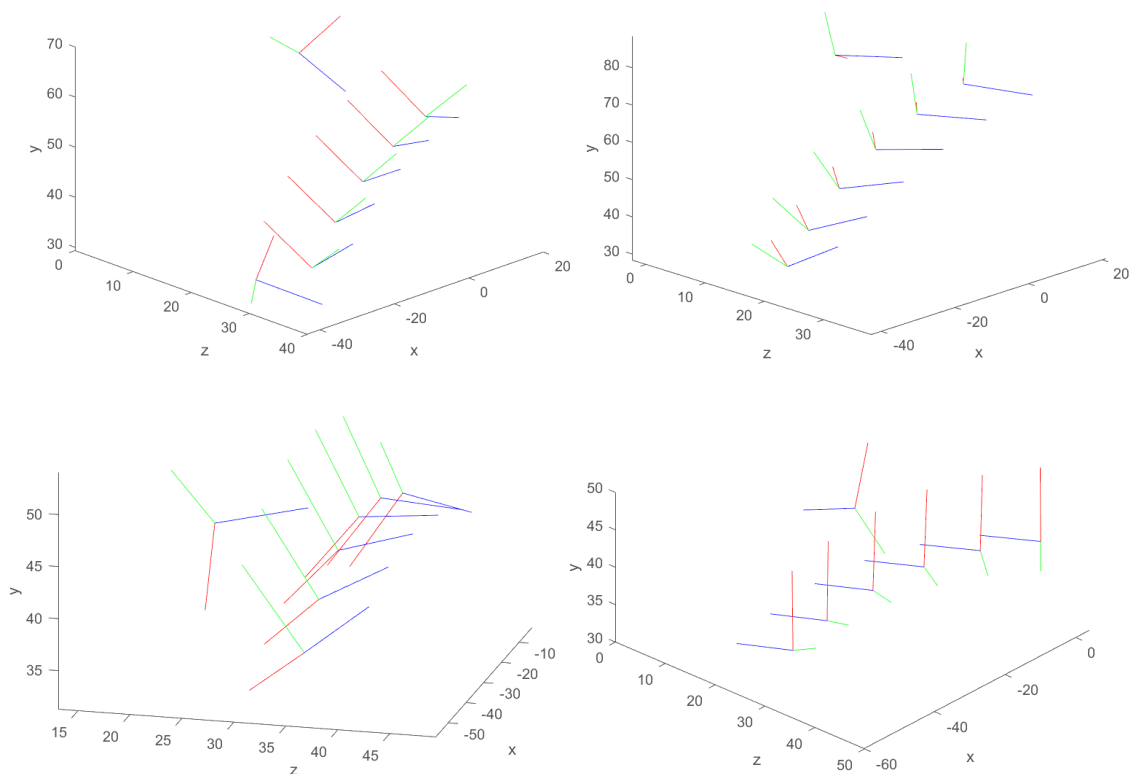
Each case is made up of eleven [D] and a total difference collected along them. When the total difference is less than a tolerance, the set of variables and distances are stored as a final candidate and a plot with the resulting trajectory of the eleven [D] is created. The tolerance is been set on $4.6e+04$.

Analysis of the results and selection of final option

Finally, all the sets of variables and plots stored as final candidates are analyzed. Based on this, the trajectory that most closely resembles it and at the same time is most useful for the gripper, is selected as the final option.

3.3.2.3. Results and conclusions

After an approximated run of the code of 8 hours, 10 solutions are stored as final candidates. The following results are obtained on their plot format.



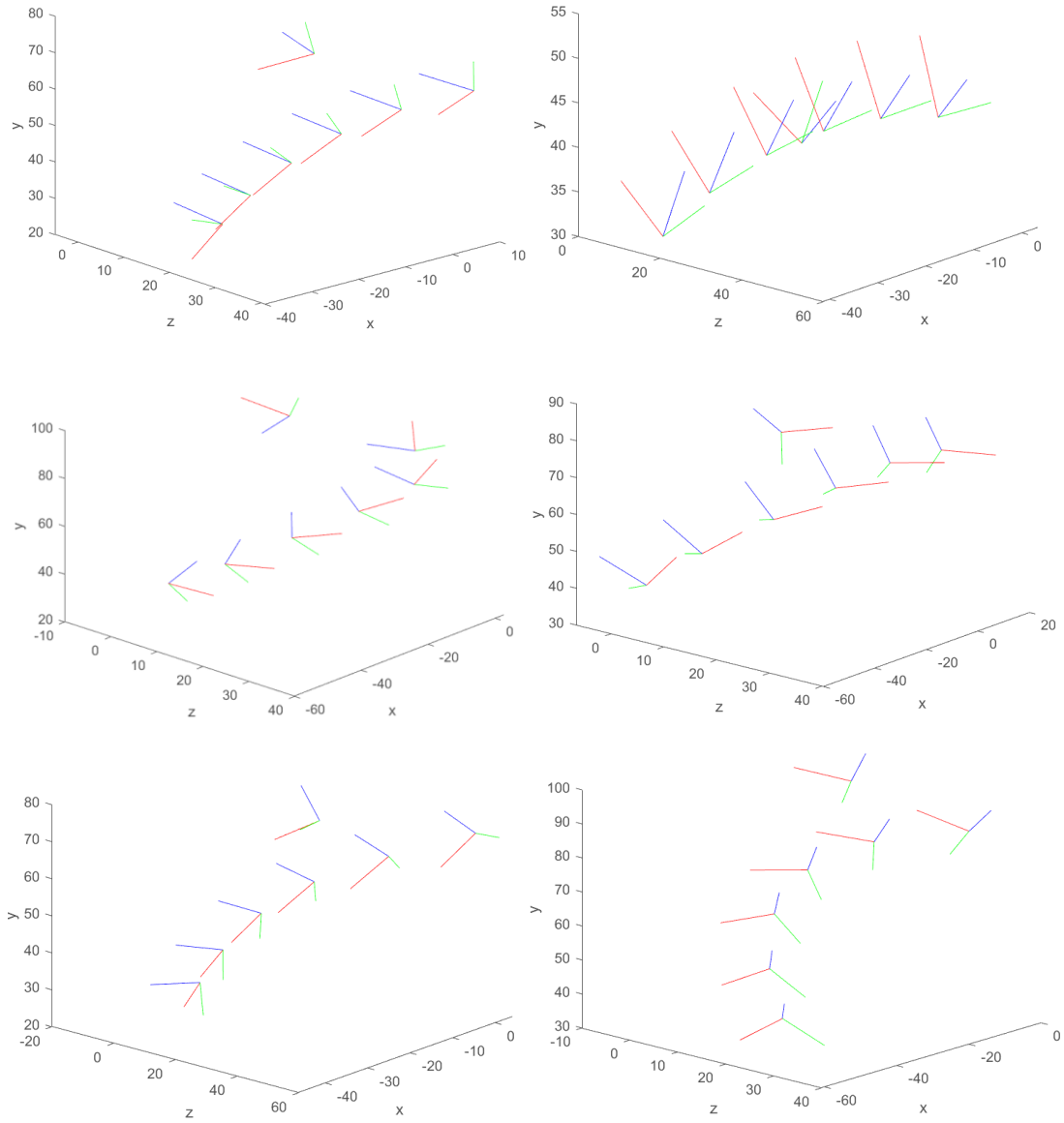


Figure 32. Collection of 10 final candidates plots

All in comparison with the ideal trajectory that as shown again in this section.

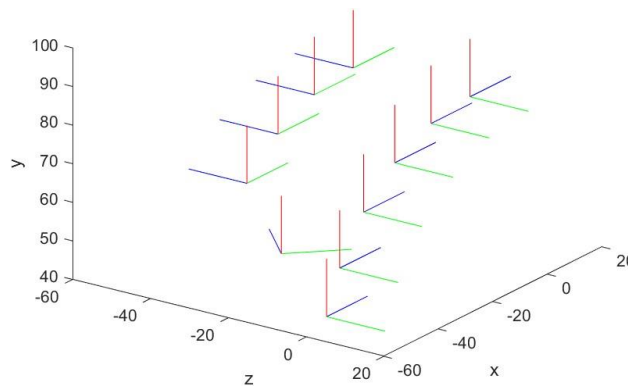


Figure 33. Ideal trajectory plot

As it is seen, the results are apparently not very similar to the ideal trajectory. Or at least, enough similar to consider them a good solution. In most cases, the mechanism is not able to perform this change of orientation necessary for the suction configuration nor the parallel grasping nor the change on z-plane. This is because on the plots seems to be less point than the studied, all the eleven points are plotted but there are many that repeat exactly the same configuration when there should be a change on the orientation and z-axis position. Besides, knowing that close loop condition was expected to impose it later and it is not imposed yet, the results are now even less sufficient as more restrictions should be done.

The difficulty of obtaining an enough good solution is a consequence of several problems. First, the high number of variables especially random makes a so complex system that creates a wide number of possibilities where search the good solution. Also, the high number of variables that are defined randomly in our case is been even more a problem. As explained, the number of equations derived from ideal trajectory allow to determine more variables by equation system solving. However, the complexity of D-H method, the b vector characterization and the high number of variables construct a so large equations to solve that are not been possible to do it by Matlab used commands. For an improvement of the process, more investigation should be done on this issue and the could would be enhanced a lot.

As mentioned on Section 3.3.2. , it must be decided if there is a continuation on the process to find the resting variables to close the loop of the mechanism. As mentioned, this will be even more restrictive and is expected to be profitable only if the results previously obtained are good enough.

Therefore, based on the reasons explained on this section, the results are considered not sufficient as there is not any candidate that is able to perform a similar trajectory than

the ideal, especially because the non-carry out by the mechanism of the change of orientation necessary for the suction configuration nor the parallel grasping nor the change on the z-axis. It is not been found any solution good enough to satisfy the task specifications.

At this point, it is considered the best idea for the continuation of this project is not to leave the objectives and try to find another method and concept to create a mechanism that fulfill task specification conditions. As it is explained in the next chapters, the new approach will study the possibility to create a system based on two different and independent mechanisms, not only one complex linkage system.

3.4. Final Approach

Also here, note that the study is centered on just one finger, the left. For constructing the entire gripper, the finger should be replicated symmetrically.

3.4.1. Structural Synthesis

3.4.1.1. Concept Design

This new approach will study the possibility to create a system based on two different and independent mechanisms, not only one complex linkage system. It is expected to be easier and possible to find a solution.

For the pinching, the idea is to use a mechanism based on one of the common parallel pinching systems.

The challenge has been to think about how to achieve the suction position when it is necessary. The concept of the final solution is to use rotatory fingers that can rotate only 90° degrees to change from pinching to suction position and vice versa. An independent mechanism included inside the gripper will act the rotation of the finger employing the relative motion between the links of the gripper. Thus, the switching between pinching and suction positions are reach using the same motor already used for the pinching movement.

3.4.1.1. Pinching system

The fingers can be configured so that their orientation with respect to the object to be gripped remains constant throughout their entire range of motion. This technique makes it possible for the inner surface of the two fingers to remain constantly parallel. This approach seeks to optimize the point of contact of the fingers with the objects, which in

turn leads to the creation of a more adaptable gripper device in different situations. Various executions of this concept are available. One of the simplest involves constructing each finger using two rods arranged in parallel. Each finger as a parallelogram four-bar linkage, is well known to keep constant orientation of the coupler.

The parallel property of the system is demonstrated by the following kinematic study.

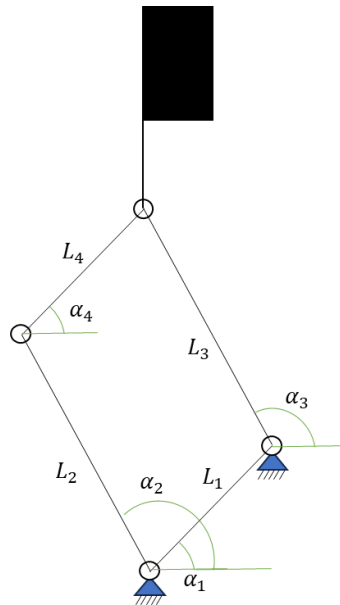


Figure 34. Schematic representation of left finger of the gripper

In the x axis:

$$L_1 \cdot \cos(\alpha_1) + L_3 \cdot \cos(\alpha_3) = L_2 \cdot \cos(\alpha_2) + L_4 \cdot \cos(\alpha_4) \quad (\text{Eq. 13})$$

$$L_1 \cdot \cos(\alpha_1) + L_3 \cdot \cos(\alpha_3) = L_2 \cdot \cos(\alpha_2) + L_4 \cdot \cos(\alpha_4) \quad (\text{Eq. 14})$$

In the y axis:

$$L_1 \cdot \sin(\alpha_1) + L_3 \cdot \sin(\alpha_3) = L_2 \cdot \sin(\alpha_2) + L_4 \cdot \sin(\alpha_4) \quad (\text{Eq. 15})$$

The interesting property comes when the parallel bars have the same length. This will be imposed and it will be demonstrated that the angles are the same between the parallel bars.

To impose this same length,

$$L_1 = L_4 \text{ and } L_2 = L_3 \quad (\text{Eq. 16})$$

Now, operating the equation for the x axis with the assumption done:

$$L_1 \cdot (\cos(\alpha_1) - \cos(\alpha_4)) = L_2 \cdot (\cos(\alpha_2) - \cos(\alpha_3)) \quad (\text{Eq. 17})$$

And for the y axis:

$$L_1 \cdot (\sin(\alpha_1) - \sin(\alpha_4)) = L_2 \cdot (\sin(\alpha_2) - \sin(\alpha_3)) \quad (\text{Eq. 18})$$

Once here, the only possibility to maintain the equality is to have a subtraction of cosinus and sinus of zero value. Or what it is the same, that the angles of the parallel bars should be equal between them.

$$\alpha_1 = \alpha_4 \text{ and } \alpha_2 = \alpha_3 \quad (\text{Eq. 19})$$

This property is so useful for the fingertip. It guarantees the constant orientation of the fingertip which is fixedly attached the L_4 bar. Besides, this fixed angle of the fingertip can be control by the relative angle (α_1) of the two articulations that are attached to the ground, the gripper casing in our case.

Once decided the structure, it is needed a source of motion and a transmission to the structure.

For the source, an electric motor is used. Their most common types are the linear motor and the rotatory motor.

In the linear motor, the actuator that opens and closes the clamp is a linear actuator. This may be a pneumatic piston. The main inconvenient of the gripper is that it is necessary a large actuator to reach a large grip width required for certain objects. This would increase notably the size of the gripper. Also, the linear actuators tend to be more expensive and more complex.

When a rotary motor is used, the most common implementation is with a worm drive reduction system. The movement is transmitted from the motor to the gears through a worm screw attached to the motor, which engages the two gears at the same time. Each finger is connected to one of the wheels and maintains its rotation. The direction of rotation of the two wheels is opposite, so that when the fingers move, they open or close the clamp. Note that this part of the finger attached to the wheel nor its parallel do not move parallelly with the ones of the other finger, it is only the fingertip which does it. A rotatory motor is cheaper and easier to control the opening of the clamp thanks to a large reduction of the wheel speed compared to the motor speed.

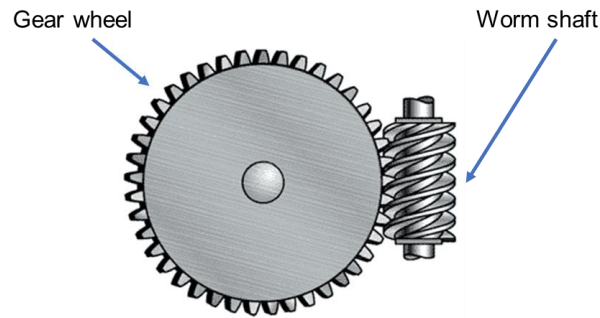


Figure 35. Worm drive [24]

Based on these mentioned advantages, the rotatory rotor has been selected for the new prototype.

For the transmission to the structure, the bar L_2 will be attached to the gear wheel. Then, the gear wheel acts now as the articulation between the solid L_1 and L_2 and the gear wheel axis becomes the articulation axis.

Therefore, the opening and closing of the fingertips are controlled by the rotation of the electric motor controlled by a controller.

3.4.1.2. Suction switching system

Suction switching system

As mentioned, rotatory fingers will be included on the gripper that can rotate only 90 degrees to change from pinching to suction position. The independent mechanism included inside the gripper will act the rotation once the pinching trajectory is finished and for 10° more (from 65 - 75° of gripper aperture as will be explained later). It is based on the following system.

First, note that there is a relative rotation between the links L_2 and L_4 . The idea is to take advantage of it to turn the fingertip. It can be seen easily from the figure, that the more opened the gripper, the lower the angle.

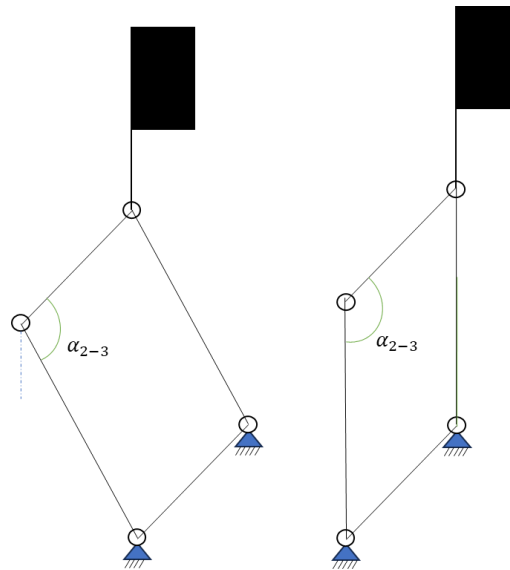


Figure 36. Finger structure on two different positions

Let us first see a scheme with the variables to understand better the mechanism.

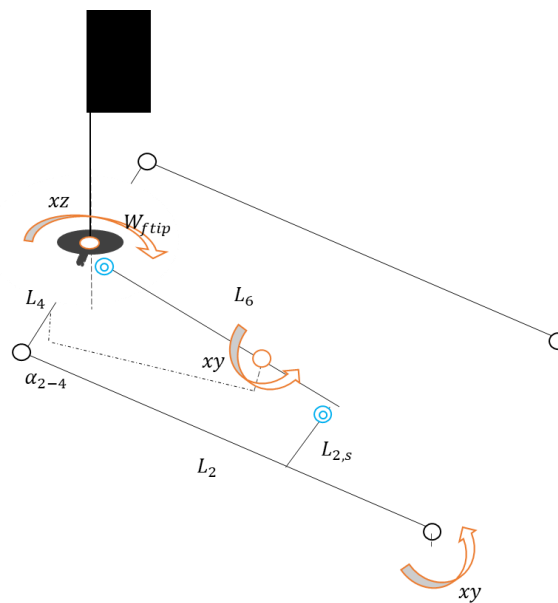


Figure 37. Suction switching system scheme with variables defined

The first part of the mechanism will be a solid attached to L_2 called $L_{2,s}$. When the gripper is opened at a specific angle, this solid will push as a cam joint another link called L_6 which is articulated to a revolute joint attached to L_4 . Note that the pushing occurs because there exists some relative rotation because $L_{2,s}$ is fixed to L_2 and L_6 is fixed to L_4 . As L_4 is articulated, so the movement is transmitted to the other end of the joint through its rotation.

And now the second part of the mechanism. This last end of the solid pushes a wheel that is solidary attached to fingertip. Then, the rotation received by the wheel is

transmitted also to the fingertip causing the turning of the fingertip. The arrival at the end of the trajectory corresponds to the rotation of 90° of the fingertip. It has only one degree of freedom that guarantee the correct working of the mechanism. The transmission follows the following scheme:

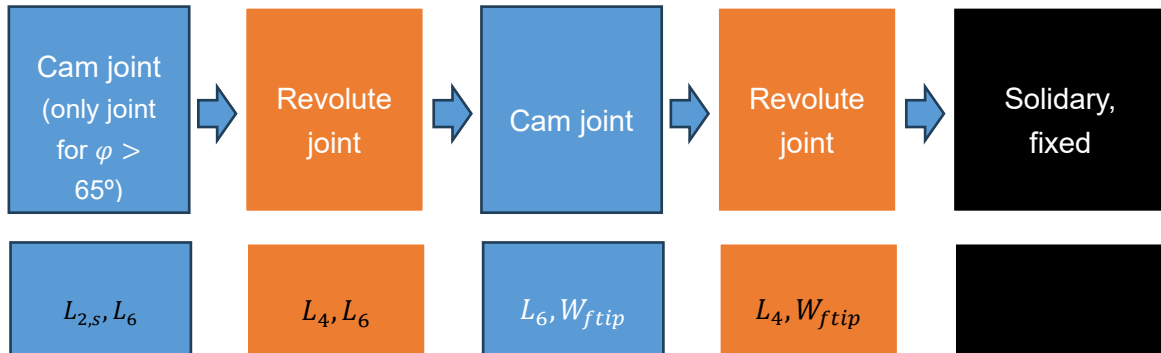


Figure 38. Kinematic pairs transmission scheme

Please see the next figure. For a better understanding, it should be noted that the representation is on 3D, the rotations occur on the plane specified on the arrow and the color of the joint coincide with the shown scheme. Also, recall that the axis of the L_6 revolute joint is fixedly attached to L_4 .

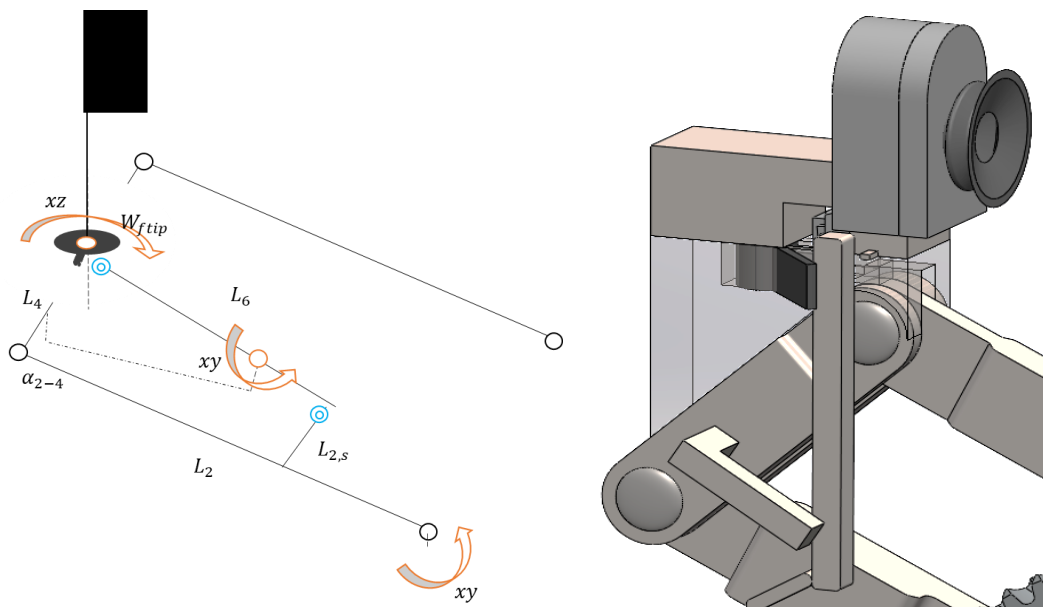


Figure 39. 3D representation of the right finger from bottom plane

Another important feature is that this mechanism will occur after all the normal trajectory of the gripper is performed. The last 10° will be reserved for this to occur, from an opening of 65° to 75° . Therefore, the dimensional design will guarantee that the switching

system starts and finishes at a desired opening angle. Therefore, the first and last cam joint only occurs on the last 10°, before there is no joint.

Besides, there is a remaining important component so important for the recovery of the positions: the springs. In this mechanism, there are two necessary springs. Although its magnitude will not be computed, they are assumed to be strong enough to complete the work specified. One will be a rotatory spring inside the revolute joint of L6. The direction of its force will be exactly the same direction as the movement of L6 also specified on Figure 39 by an arrow, but in the opposite direction of sign. The spring should be able to rotate the bar L6 to recover its initial position. Note that in the 3D design a protuberance is created on the support of the fingertip to stop this rotation made by the spring and keep it always in the initial position. And also, the axis of the wheel should have a rotatory spring that also is in the same direction but opposite sign as the spin for the switching (arrow on the Figure 39). It is also important because the spring will make the wheel to recover its position (pinching configuration) when there are no bar pushing or locking system actuating.

Fingertip locking system: "Assembly M"

Also, the system has a mechanism that locks the position until the clamp reaches its maximum opening again. From now on, it will be called "Assembly M". This is solved by the following way.

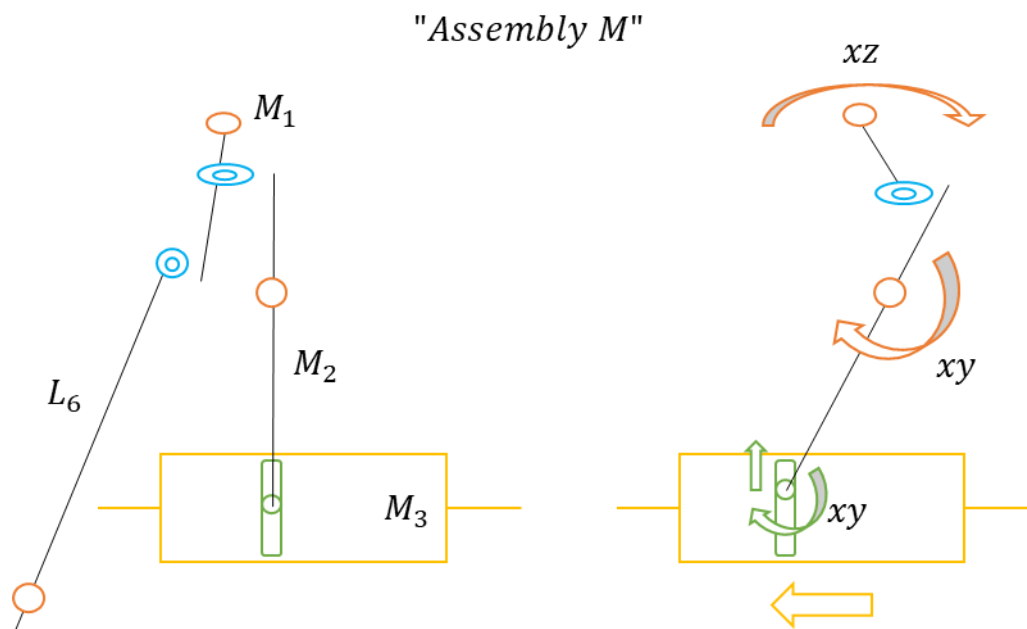


Figure 40. Structural sketch of the locking mechanism

First, consider the notation of the solids denoted on the figure. Then, take the natural and normal position the moment where the solid M_3 is inserted into the wheel by the means of a spring that pushes into it.

This natural position starts to change when the bar L_6 contacts the solid M_1 because of the following process. The idea is that the mechanism converts a rotational motion given by the bar L_6 to a linear movement of a the solid M_3 which acts as a locker of the wheel. When L_6 contacts the solid M_1 , the rotational motion is transmitted but changing its plane. Now, the solid M_2 articulated on a revolute joint, uses this motion to transmit it also to another articulated solid joint by a pin-in-slot, which again change the plane of rotation. Thanks to this joint and the two degrees of freedom, only the linear displacement is transmitted to the final solid M_3 . Also, recall that the pin-in-slot could be contemplated as the sum of a prismatic and revolute joint.

Once all this transmission is performed, the piece M_3 moves backwards and retires itself from the inside of the wheel thus releasing its spin. When all the suction switching process is finished and the bar L_6 goes backwards, the wheel recovers its position by the means of a strong spring on its axis. Then, the piece M_3 is inserted again pushed by its spring locking the rotation of the wheel. It has only again one degree of freedom that guarantee the correct working of the mechanism. Again, the transmission of the motion can be resumed on a scheme.

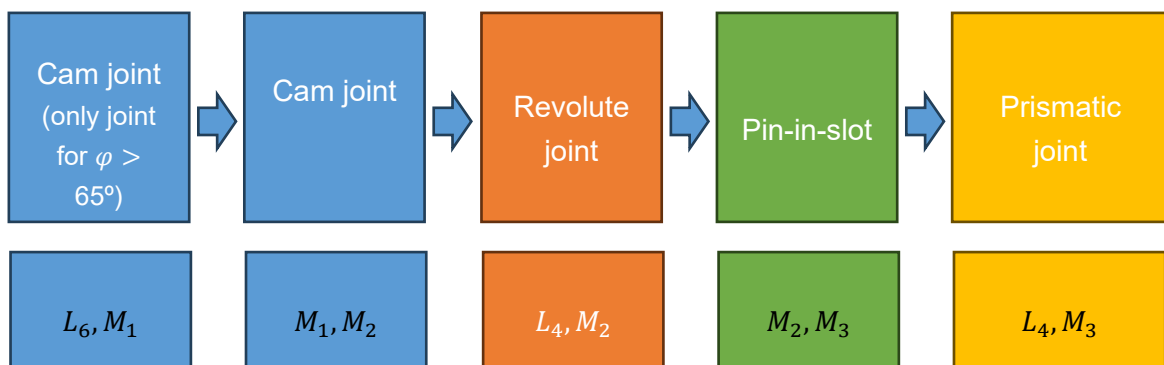


Figure 41. Scheme of the motion transmission of the locking system

Please see the following final picture of the mechanism for a better understanding.

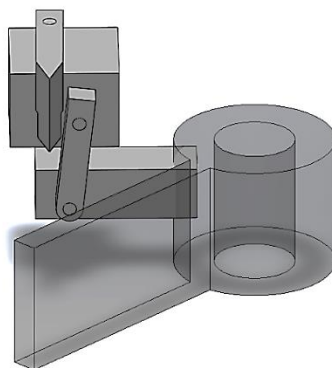


Figure 42. Picture of the mechanism on the final 3D design

Besides, there is also another mechanism of locking. It ensures that the fingertip is kept constant on all the gripper's trajectory when the suction position is selected. It consists on a hook attached to the rightmost face of the tooth of the wheel and a "Mini Push-type Catch Latch" compact system.

This system is a commercial mechanism that ensures normally a door of a cabinet is automatically opened by simply applying pressure to the door itself, thus activating the release spring in the fitting. And when the door is closed and the system is pushed again, the hook is locked and the door is closed.



Figure 43. Commercial mini push-type catch latch

And the same principle is applied on our mechanism. In this case, the door will be the wheel and the other part will be the wall of the gripper. Then, when the switching mechanism is activated, the wheel will push the latch when it arrives at the final of the 90°. Then, the suction position will be locked and the gripper can make all the closing and opening trajectory with the cups being horizontal. And when user wants to change, the switching suction system will be activated again. Now the bar L_6 will push the will on the final of the trajectory, the hook and the rotation of the will be unlocked. Then, the wheel and the bar return to their natural position through their springs.

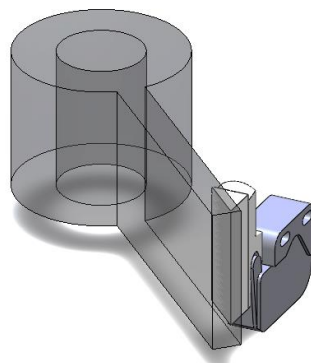


Figure 44. Picture of the mechanism on the final 3D design

It is decided to include the compact commercial form of the latch on the design. The main reasons are the complexity of the mechanism and the small dimensions and the accuracy that should have the solids inside. At least as a first design, it is been

considered that the mechanism will operate more reliably using a commercial compact one.

Finally, both mechanisms are combined to lock the position of the wheel for pinching or suction configuration.

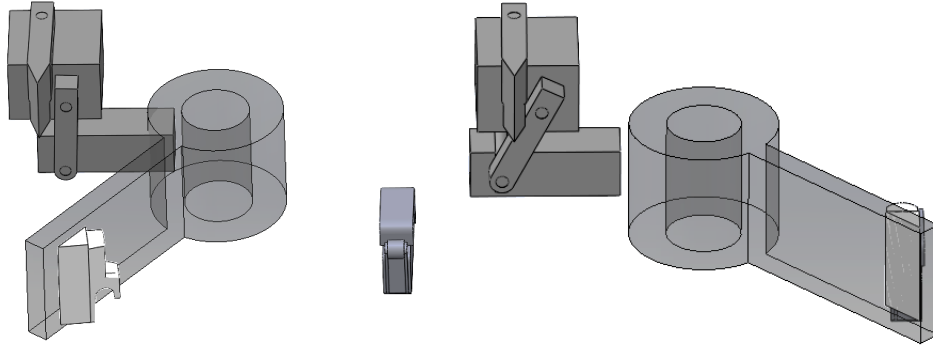


Figure 45. Pictures of the first and last positions of the complete mechanism on the final 3D design

As commented, here it will be also necessary a spring. In this case, linear. It should be allocated behind the solid M3 and should push them to try to insert the flange on the wheel. In this manner, when the wheel is on the natural position the flange is automatically inserted into it because of the wheel hole.

3.4.2. Dimensional Synthesis

3.4.2.1. Pinching system

Let us find the most appropriate dimension of the components of the fingers. The figure will help us to understand the variables and the mechanism.

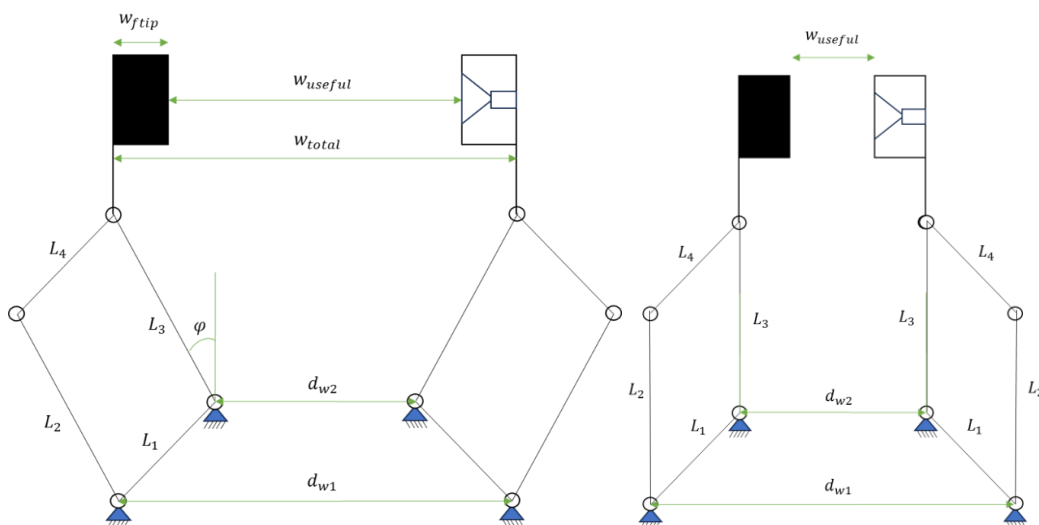


Figure 46. Structural schemes of the pinching system with dimension variables

As studied in the Section 5.2.1., the desired width of the pinching dimensions is $w_{useful} = 110 \text{ mm}$. But in this prototype, there are suction cups on the surface of the fingertip that reduces the useful width of the clamp. This reduction is estimated on 12.5 mm per finger [20]. Then, the w_{total} should be of 135 mm at minimum.

Also, the activation of the finger rotation mechanism should be activated on the last part of the opening. Because it is wanted a quickly but not too hard mechanism, it is decided to reserve the last 5° to allow to occur this mechanism. Note that this consideration does not effect on the maximum opening for pinching because this 10° are only used to switch the position but no grasping. However, the contemplation is important if there is a mechanical locking system not to overpass the maximum opening.

For the calculation of all the parameters, the common gripper OnRobot RG2 will be a reference for some of them. After that, the remaining values will be computed in order to satisfy our particular case. Also, there will be a revision to ensure that the reference values allow us to get a feasible solution.

The variable d_{w1} are determined by the distance of the gears moved by the wormed screw attached to the motor and is approximated on $d_{w1} = 69 \text{ mm}$. Also, the variable L_1 and L_4 also defines the configuration of the structure and are estimated on $L_1 = L_4 = 30 \text{ mm}$.

For the definition of d_{w2} let us introduce the following reasoning. It is so interesting that the maximum height of the fingertip trajectory (maximum position on y) is achieved in the exact moment of the closing of the gripper. This provides the prototype two properties. Firstly, the combination of the trajectories of the surface of the both fingertips become perfectly circular, an advantage for the easier intuition and calculation of the trajectory that will follow the gripper. Besides, it makes the gripper more competitive in situations where the object is small or difficult to reach because the grasping occurs on the largest height. This last feature could represent an advantage in particular cases with respect to the common OnRobot or Universal Robots RG2 products, where the grasping occurs a small instant later [20] [3]. To understand it, imagine a small flat object resting on a flat surface like a table. If the closing occurs later than the maximum height, the collision with the flat surface on the y axis could occur before the clamp is closed and would cause the closing occurring in a lower height. This lower height could be insufficient to reach the object and become impossible to grasp it. Returning to the variable d_{w2} , this states the distance between the axis of the articulations. And with this parameter it is possible also to achieve the property explained. Then, for the determination of the parameter the following condition is applied using the variables of the Figure 46.

$$w_{useful} = 0 \text{ mm} \quad (\text{Eq. 20})$$

$$2 \cdot L_3 \cdot \sin(\varphi = 0^\circ) + d_{w2} = w_{ftip} \quad (\text{Eq. 21})$$

$$d_{w2} = 2 \cdot w_{ftip} = 25 \text{ mm} \quad (\text{Eq. 22})$$

Therefore, $d_{w2} = 25 \text{ mm}$.

Finally, let us state that the maximum opening configuration is achieved by an angle of $\varphi_{max} = 65^\circ$. This limit must be set in order to avoid the collision of the object with the gripper's body, something that could be more probable with a lower angle.

And now the remaining variables $L_2 = L_3$. Besides, the maximum desired opening $w_{total,max} = 135 \text{ mm}$ and the angle $\varphi = 65^\circ$ are the variables which will define them by the following equation.

$$2 \cdot L_3 \cdot \sin(\varphi_{max} = 65^\circ) + d_{w2} = w_{total,max} \quad (\text{Eq. 23})$$

$$L_3 = \frac{110 \cdot 3^{\frac{1}{2}}}{3} \approx 60.7 \text{ mm} \quad (\text{Eq. 24})$$

Finally, let us resume the values defined for all the parameters of the prototype in the following table.

Table 8. Final parameters summary

L_1	L_2	L_3	L_4	d_{w1}	d_{w2}	$w_{total,max}$	$w_{useful,max}$	φ_{max}	$\varphi_{suction}$
30 mm	60.7 mm	60.7 mm	30 mm	69 mm	25 mm	135 mm	110 mm	65°	65°-75°

In addition to schematic dimensions, the width and depth dimensions are also important for the sizing of the structure. The industrial drawings of the parts with the 3d dimensioning are shown below. It should be noticed that all the width and depth are decided based on the RG2 Robot in order to ensure a correct operation of the gripper.

The solids L1, L2, L3 and L4 are assembled in the following manner.

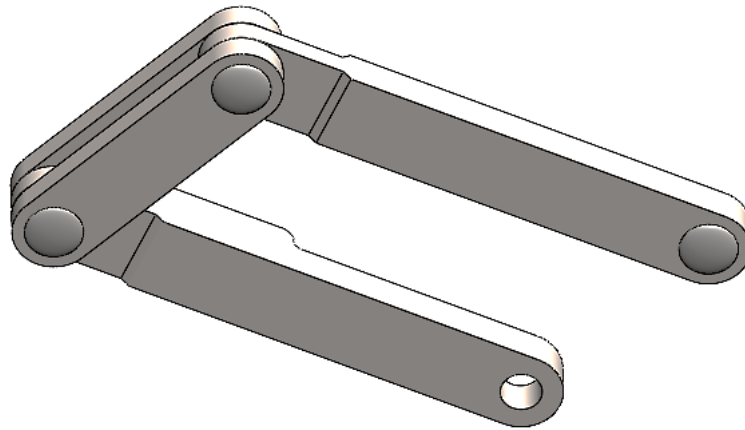


Figure 47. One finger assembly of L1, L2, L3, L4

The L1 is a symbolic solid made by the fixing its ends on the gripper casing. Then, has no volume.

The L2 and L3 industrial drawings are shown below. The assembly requires two of this part for each finger and for four the total gripper.

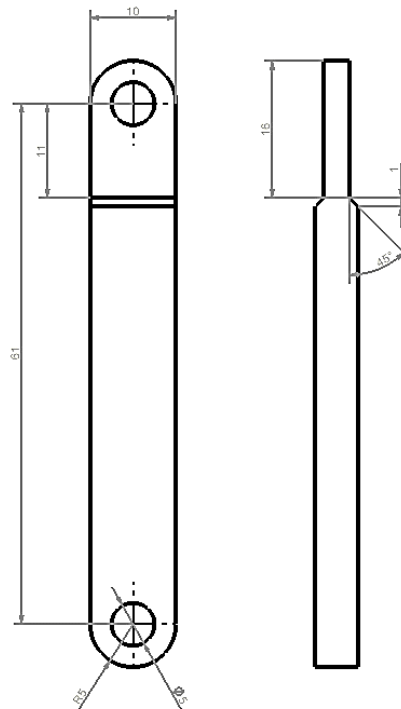


Figure 48. L1 industrial drawing

The L4 will be constructed on two bars of the following dimensions. For the entire gripper, four bars are required.

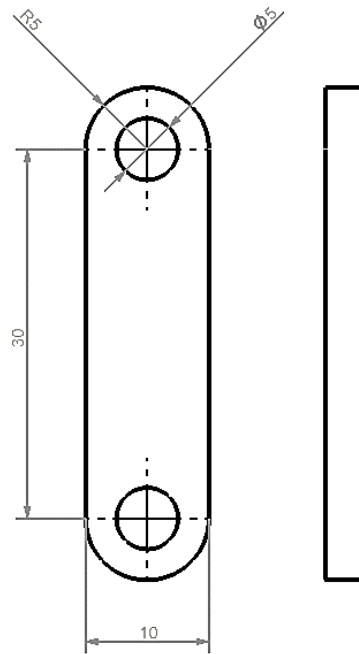


Figure 49. L4 industrial drawing

Some small changes may be done on the final parts to fit the mechanism that should be included on the detailed design.

3.4.2.2. Suction switching system

A dimensional graphical study using SolidWorks software is performed on both switching system to determine the shape, sizing, and position of the parts. In the following sections, the process followed is explained.

Suction switching system

The section is explained on different steps to make it more understandable.

Explanation of components

First it is necessary to explain that a support for the fingertip will be added. This is in order to create a support that allow a planar rotation of the fingertip. It is solidary to the solid L4 and does not rotate. It should be noticed that coincide with solid L4 dimensions. However, there are changes that are necessary to consider it for the design in detail. These are related not to collision with other parts of the gripper and to allocate the axis of the wheel and the locking mechanism. Now the basic external dimensions will be shown as they are the necessary for this moment.

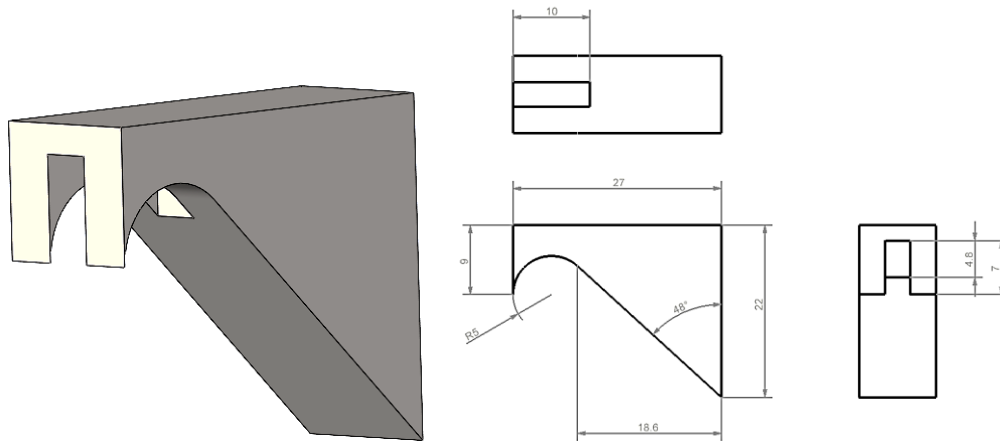


Figure 50. L4 component

And also, it is constructed the rotative fingertip. It has the following specifications. It is only an orientative fingertip because some changes should be made when make the detailed design, as the holes for the air cables, the slots do the fingertip to adapt and catch better, the thread and other features. In the same manner, an orientative suction cup cover is created on the 3D.

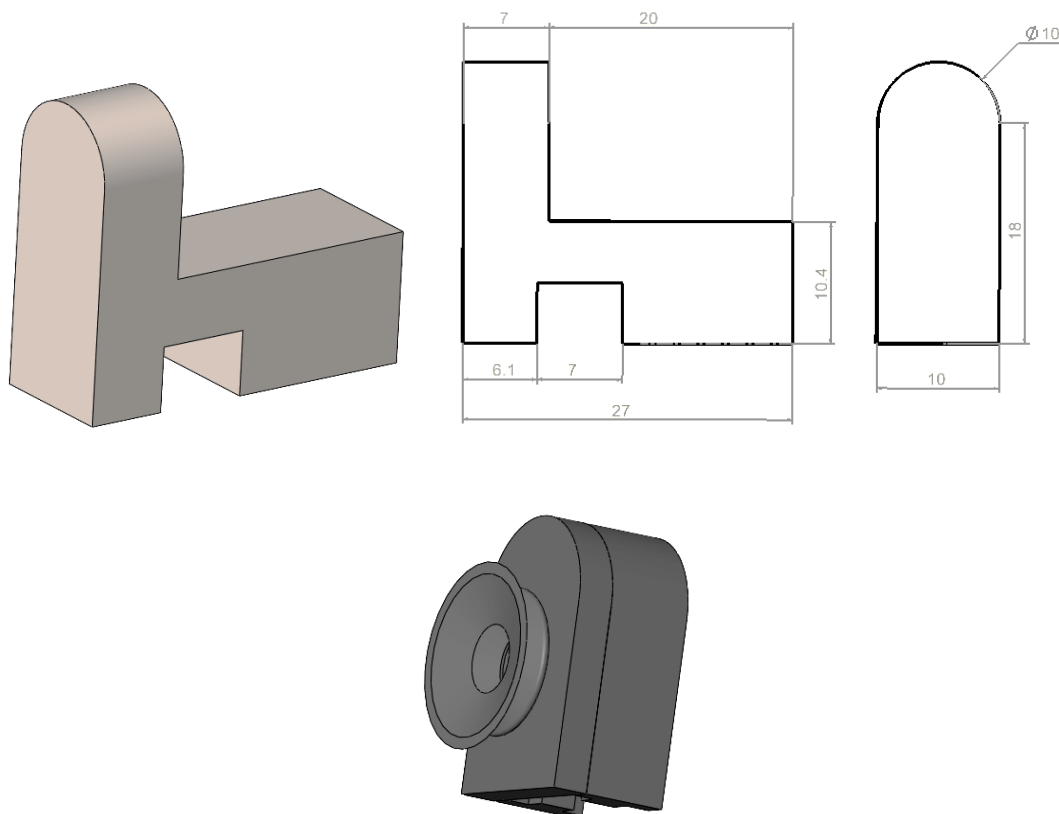


Figure 51. Rotative fingertip and suction cup cover

To have a notion, these parts are assembled on the following way on the gripper.

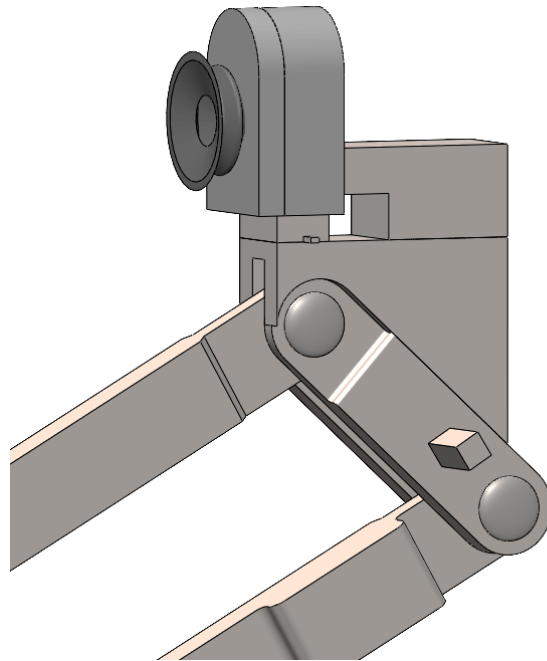


Figure 52. L4 and fingertip assembly

Definition of the Wheel7 dimension

The first done it has been to decide the dimensions of the fingertip wheel.

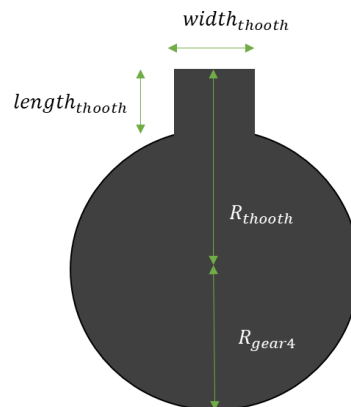


Figure 53. Fingertip wheel dimensions

Firstly, let us recall that the wheel must do a rotation of 90° to rotate the fingertip. It is decided to do it from 45° to 135° with respect to the lateral plane of the fingertip. This is because it is the most optimal way to ensure an easy contact with the solid L6.

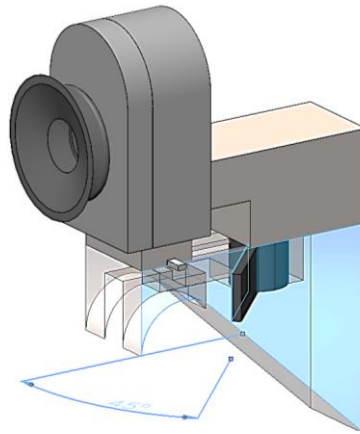


Figure 54. Fingertip assembly constraint

For the teeth, note that the bar L_6 is the responsible to contact the teeth to rotate the fingertip. In order to ensure that all the bar does not surpasses the dimensions of the teeth, the length of teeth must be large enough. Besides, another consideration has been made. The smaller the length of the tooth, the less displacement must be done by the solid L_6 to rotate it 90° and the better for the design.

Taking all these considerations into account, the following wheel has been constructed. Also, it is constructed a proportionate tooth and wheel so as not to be worn. Therefore, its final dimensions are the shown below.

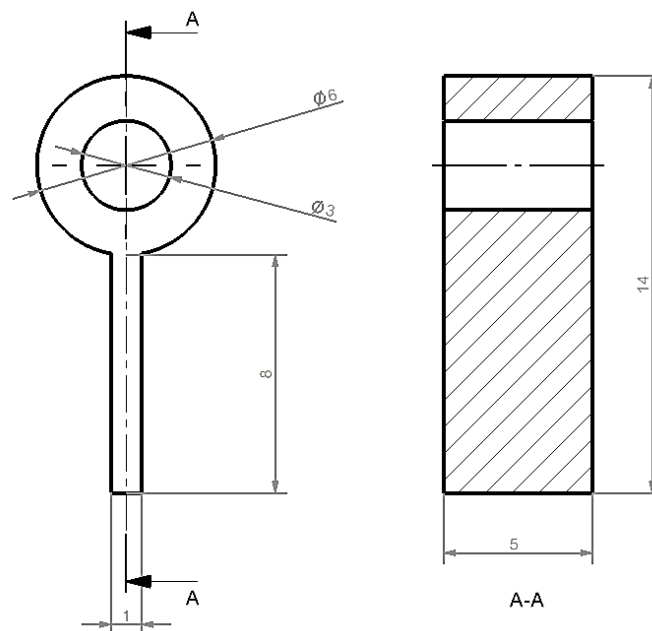


Figure 55. Fingertip wheel industrial drawing

Also, specially for the consideration because of the consideration of reduce the tooth diameter, the wheel axis is decided not to be aligned with the center of the fingertip. Besides, this is imposed because to make the suction cup fingertip surpass all the lateral

volume of the gripper and avoid to be an obstacle when grasping objects. This is its position with respect of the bottom of the support of the fingertip.

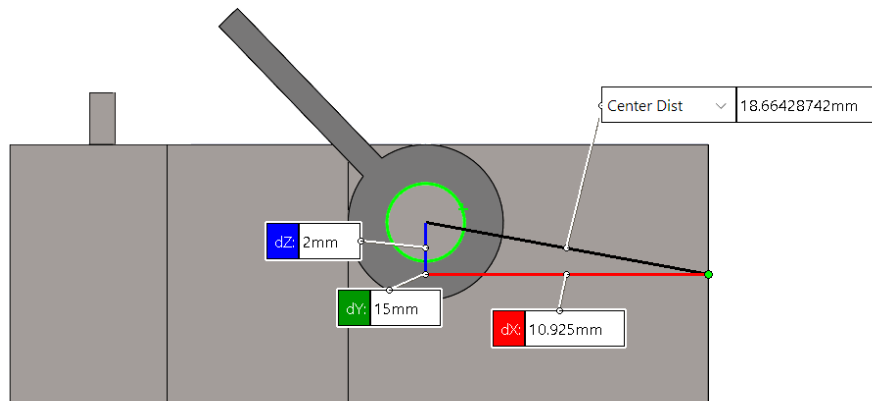


Figure 56. Fingertip wheel assembly dimensions

Definition of the L6 dimension and position

Once the wheel is fixed, now it is the moment for the definition of the solids L6 and L2S. First, let us take a look on the assembly with the wheel to understand it better.

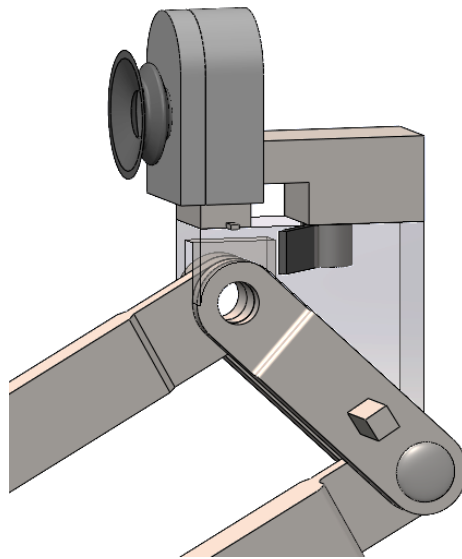


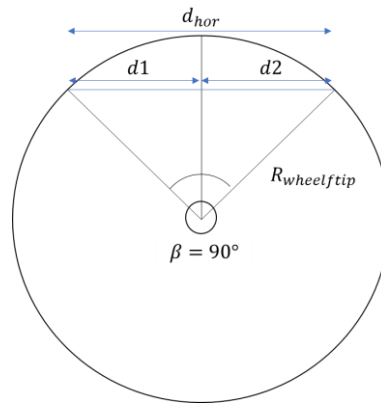
Figure 57. Assembly with the wheel

The interesting idea is to study the variables when the mechanism is activated. Before than that, the solids do not move with respect to the gripper. Let us define the variables involved. The initial and final angles where the mechanism start and finishes are the following.

$$\varphi_{ini,suction} = \varphi_{max} = 65^\circ, \varphi_{final,suction} = 75^\circ \text{ and } \varphi_{range,suction} = 10^\circ$$

The goal is to construct a mechanism that activates the rotation of the fingertip when the wheel is in the initial position and rotate it 90°. Note that the mechanism should still pushing the rotation when the 90° are done, it is the motor that prevents the rotation from continuing to occur by stopping.

First, a study has been made to know an approximation of the relative horizontal displacement that L6 has to do to push the wheel until the end. To do it, a radius of 7 mm is considered as it is the middle point of the tooth. And with it, horizontal component is obtained based on the following figure and equations.



$$d_{hor} = d_1 + d_2, d_1 = d_2, d_{hor} = 2 \cdot d_1 \quad (\text{Eq. 25})$$

$$d_1 = R_{wheeltip} \cdot \sin(45) \quad (\text{Eq. 26})$$

$$d_{hor} = 2 \cdot R_{wheeltip} \cdot \sin(45) = 2 \cdot 7 \cdot \sin(45) = 7\sqrt{2} \cong 9.9 \text{ mm} \quad (\text{Eq. 27})$$

Using this as the main guideline together with the dynamic analysis of the system on the 3D design, the following dimensions and position for the solid L6 and L2S are determined.

For L2S,

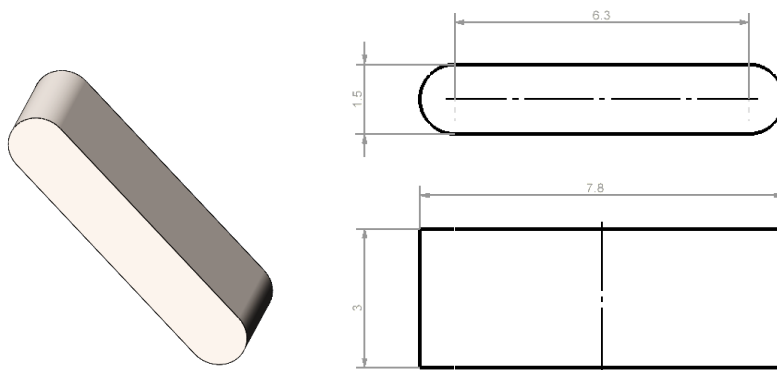


Figure 58. Industrial drawing of the L2S dimension

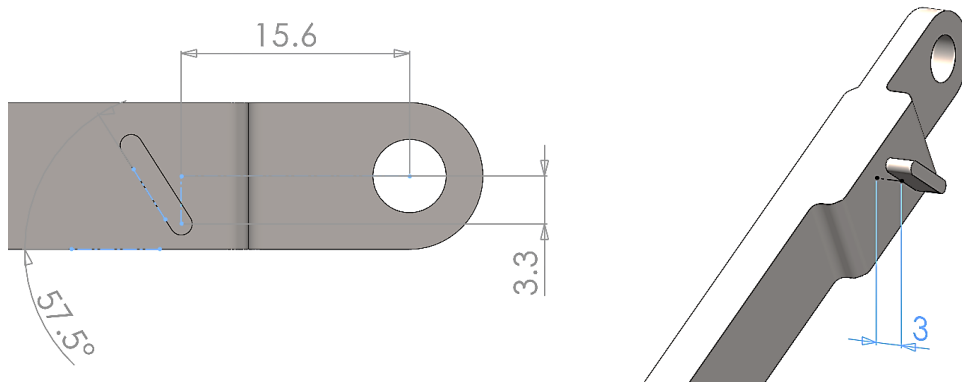


Figure 59. Position dimensions of L2S with respect to L2. Note that is L2S is totally fixed with respect to L2.

For L6,

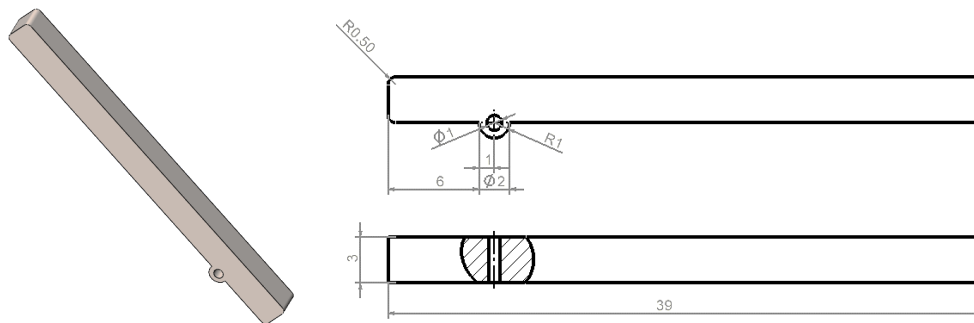


Figure 60. industrial drawing of the L6 dimension

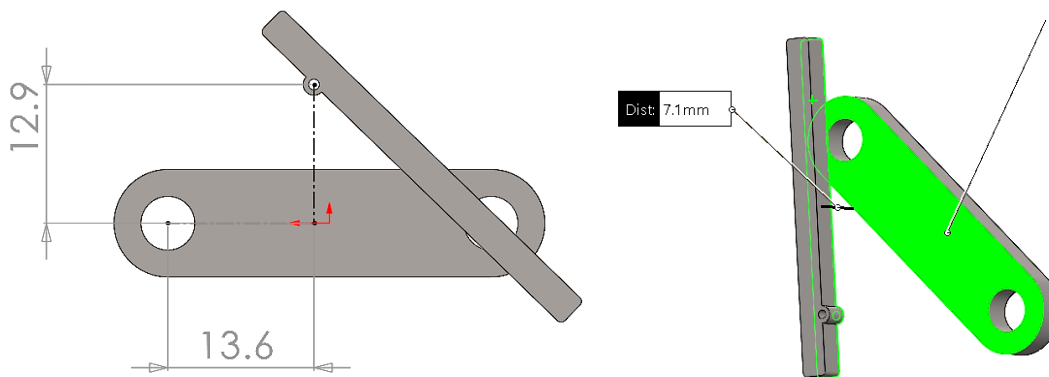


Figure 61. Position dimensions of L6 with respect to L3. Note that only the axis is fixed to L3 but no all the part

Finally, let us look some pictures of the final assembly.

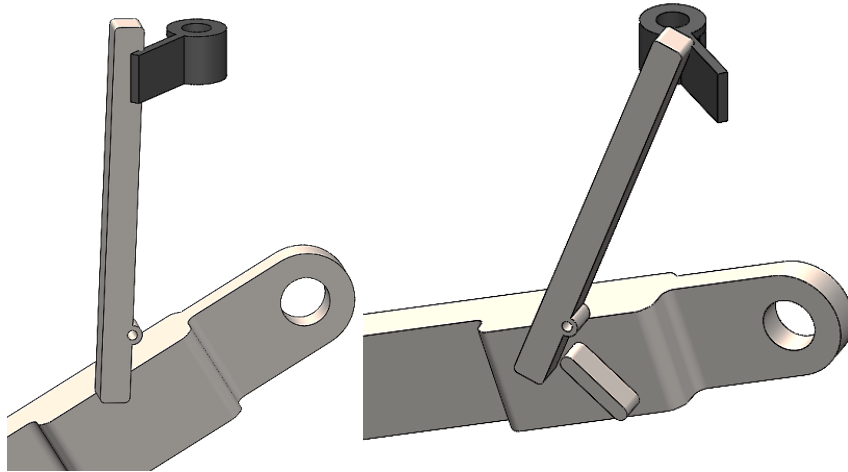


Figure 62. Final assembly representation

In the 3D design, the axis of the L6 revolute joint has been fixed to the bar L4 in the following way. This part is not specifically dimensioned because it is only a functional part with no specific shape only created for the 3D design to make sense. However, the real shape will be done in a further continuation of the project on the detailed design.

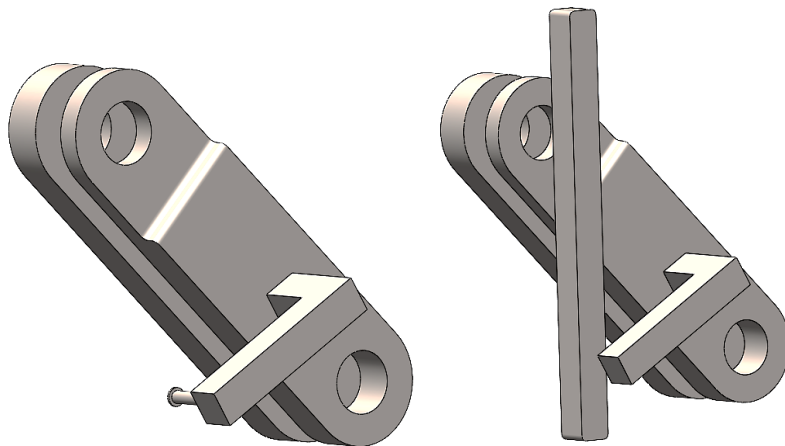


Figure 63. L6 attachment representation

Fingertip locking system: “M assembly”

This section is separated into steps to make it more understandable.

Main consideration: available space and non-reduction system

The definition of the available space is constrained by the L_4 bar, the fingertip wheel, and the fingertip. It is estimated a cube of 10x10x10 mm of available space. This will serve as a guideline to limit the dimensions of the locking system.

In addition, there is another parameter to consider that is very likely to mark this design process. The idea is to make a small mechanism that unlocks the wheel quickly. The problem is that for it to be fast, the trajectory where L6 actuates the mechanism must be short. But at the same time, you must have the flange removed from approximately inside the wheel. So, during all the dimensioning, this will be considered and we will try to increase or not to reduce the linear trajectory of the bar L6 with respect to the one that will have the flange M3, while satisfying all the other parameters.

Based on these two main considerations, the dimensions of the parts corresponding to the left finger are the explained below. The same parts but symmetric have to be replicated to obtain the entire gripper.

Definition of M1 dimensions

For M1, it is remarked that it has two cam joints on its surface, so it is intended to be as larger as possible. Also, the rotation direction should be conserved and the hinge joint should be as far as possible from the cam joint with M2 so as not cause a reduction effect. This is the resulting and the corresponding dimensioning of the M1 part. Besides, an arrow shape has been applied to make easier the surpass of the solid L6 in a certain moment.

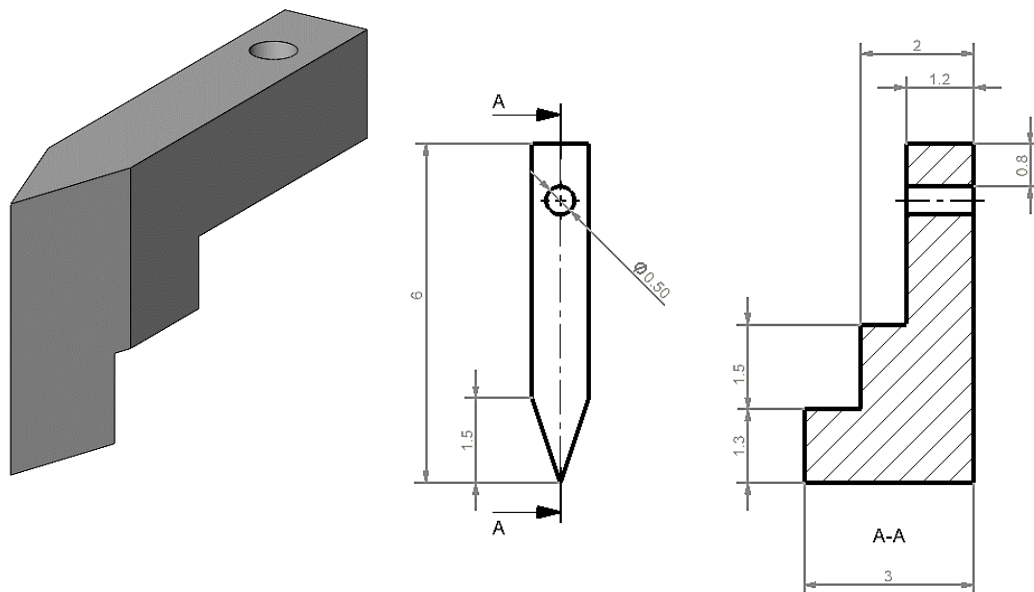


Figure 64. 3D picture and industrial drawing of M1

Definition of M2 dimensions

For M2, the part is again intended to be as larger as possible and with a revolute joint should be as far as possible from the pin-in-slot with M3. This is to pursue the mentioned aim to increase as much as possible the linear horizontal trajectory

transmitted to M3, that should be sufficient to remove the flange from inside the wheel. Here there are the picture and the dimensions.

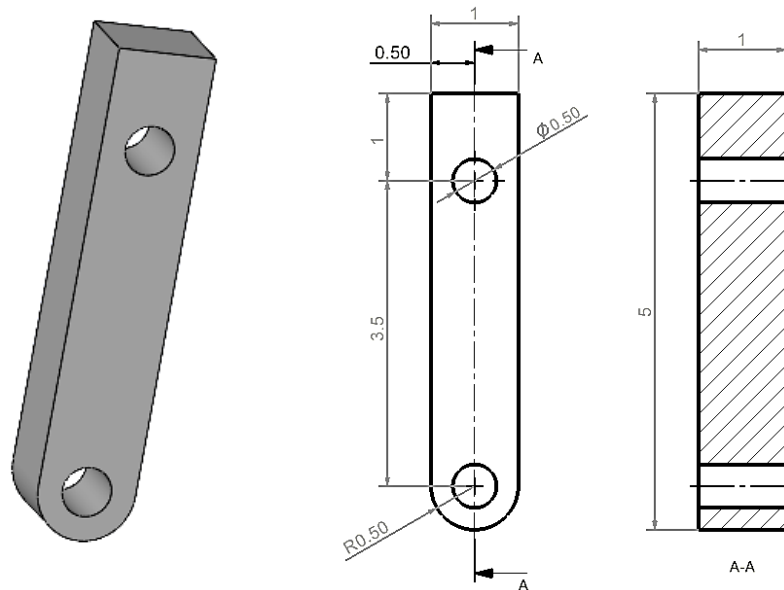


Figure 65. 3D picture and industrial drawing of M2

Definition of M3 dimensions

For a correct operation of the locking of the wheel, the effective flange that should be inserted into the wheel is estimated to have a horizontal length of 1-1.5mm. Also, for this part, all the possible remaining vertical available space will be used for the height of the part. It is important to avoid that M1 rotates too much enough to surpass the height of the pin-in-slot cavity and separate. Then, the higher the part, the less restrictive become. Finally, the cavity is located on the left so as to leave enough space for the flange.

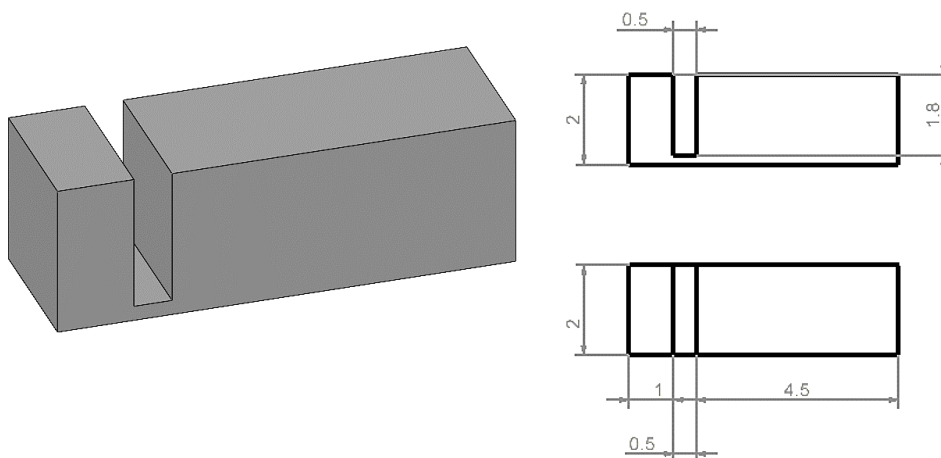


Figure 66. M3 dimensions

Definition of the position of the assembly M on the gripper

It is important for the mechanism to work only when it is necessary. To do it, a graphical study has been performed in order to find the relative position of the mechanism in the assembly with respect to the solid L6 that is already fixed.

First, a desired trajectory of the flange of 2mm has been imposed. The first and natural position of it is when this is parallel to the vertical plane. And its position on the backward configuration is found by imposing this 2 mm setback by a sketch on Solidworks.

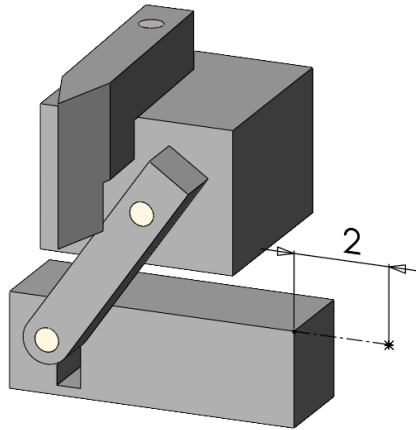


Figure 67. M assembly constraint

Later, the “Collision Detection” of the “Move Component” function of Solidworks is used to detect when the collision is produced. This is the point where the solid L6 should finish its contact with the M1 solid and surpasses it. As L6 is moving through a horizontal displacement of L6 seen from the top view, as M1 is making a rotation, there is a point where L6 finishes to push forward M1 as surpasses it.

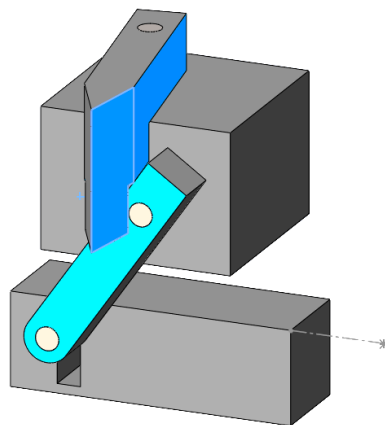


Figure 68. M assembly collision detection

Once obtained the configuration, the top view is selected. By the means of “Convert Entities” tool, the silhouette of M1 is projected on the plane on the starting and final

position of the operation. Now, the distance between the axis and the end of the arrow on the both configurations. As the solid L6 must release its contact just at the moment of the final configuration of the mechanism, where the flange has receded 2 mm.

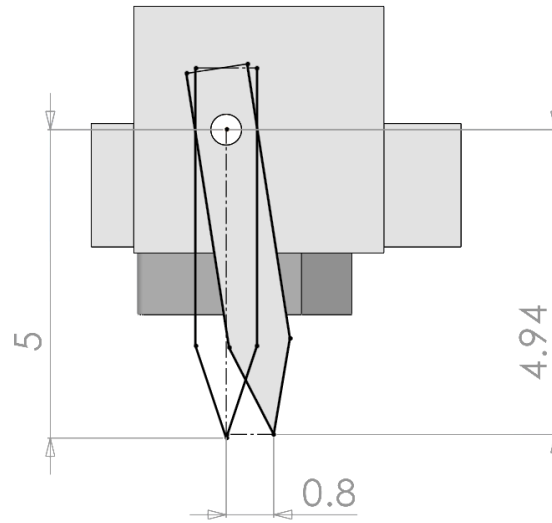


Figure 69. M assembly vertical and horizontal displacement

And it is found the relative position of the mechanism with respect to the solid L6. Its axis must be at 4.9 mm of perpendicular distance to L6.

Also, the horizontal optimal position of the M1 axis with respect to the wheel axis has been set imposing some conditions. It is important that that L6 starts contacting the wheel once the flange is already released. Then, the flange should be released before the end of contact between M1 and L6. Also, at M3 has to recede a little bit more than necessary for the wheel to has some margin to spin freely and reduce some possible operation problems. To satisfy it, this is the horizontal position selected for the mechanism based on the imposition of having a flange inserted to the wheel of 1 mm.

First, it is checked this condition of 1 mm inserted on the wheel on its natural position and that L6 is no pushing the wheel yet. Both conditions are verified by the pictures below.

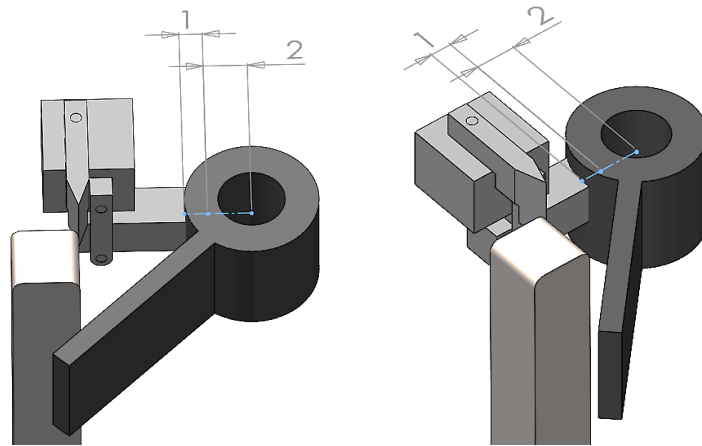


Figure 70. 3D conditions verification

Finally, it is checked that when the contact with the wheel is reached, the wheel is far enough from the wheel. And it is also checked that the backlash of M3 is not totally completed when M6 touches the wheel for the first time. The pictures below, where the components are at the same position, both conditions are also verified. There is 0.58 mm that separates M3 from the wheel. As the total trajectory that M3 is imposed to be 2 mm, and in its initial position is at 1 mm inside the wheel, it is easy to see that it has 0.42 mm yet to move until it reaches the most setback position.

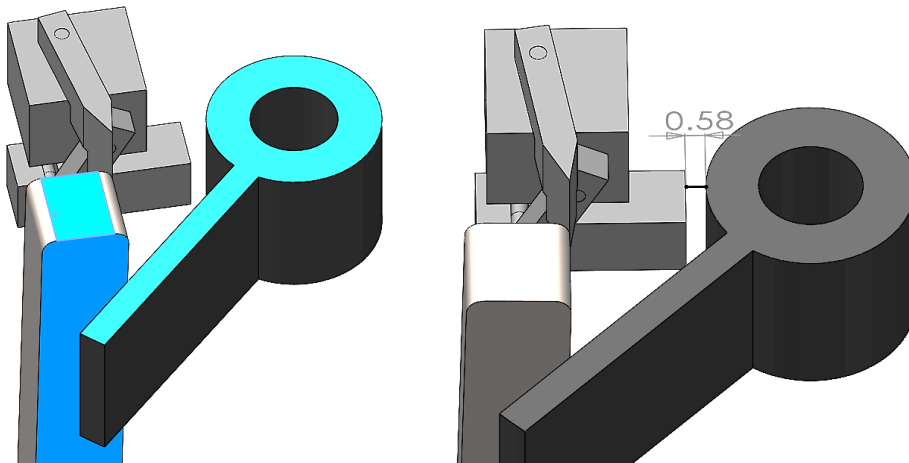


Figure 71. Conditions verification

Also, when all the dimensions are decided, a hole into the wheel has been made for the flange to enter. It is of the following dimensions with a depth of 1 mm as computed. Note that some margins are applied on the dimensions of the hole to reduce possible operation problems.

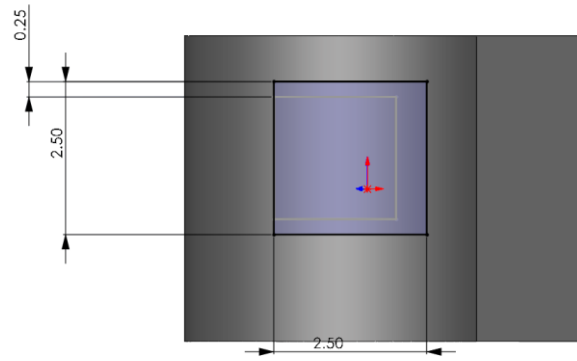


Figure 72. Wheel hole

Definition of the position of the latch

The hook of the latch has intended to attached as external of the wheel as possible. Because farer from the axis of the radius, larger the trajectory tour by the wheel and the hook and better will work the mechanism of catching the hook by the latch. The hook is putted centered on the height and at 1 mm of the end of the wheel. According to this, it is located the latch fixed on the L4 solid. However, this can be considered a guideline as the final dimensions will really determine the final position.

Here it is shown a resume of ones of the main important measures obtained and the final assembly of the mechanism.

Horizontal trajectory of M1	Horizontal trajectory of M3	Effective flange	Horizontal separation when L6 start to contact Wheel
0.80 mm	2.00 mm	1.00 mm	0.58 mm

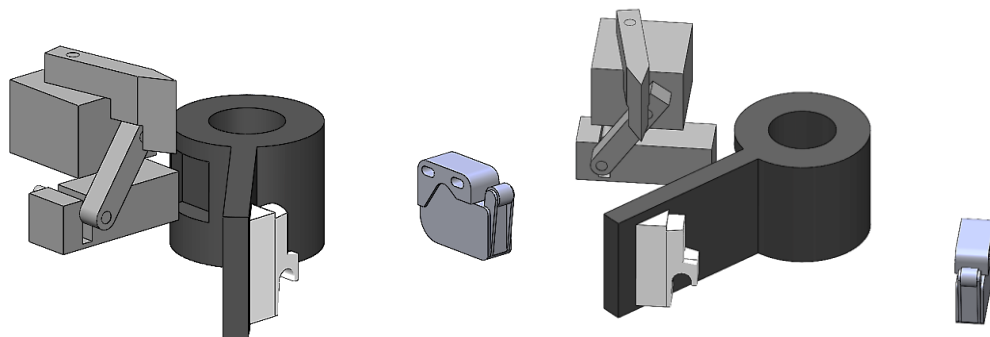


Figure 73. Entire locking mechanism representation

3.4.2.3. Reduction system

Firstly, it is important to define the closing time (t_p) of the gripper. For the purpose of designing the most competitive gripper, the t_p is set based on an experimental estimation of the closing time of the gripper OnRobot RG2 [2]. Then, $t_{cl} = 0.5 s$.

Note that it is the same that the opening time and both equal to the half of the total time of a cycle.

$$t_{cl} = t_{op} = \frac{t_{cycle}}{2} \quad (Eq. 28)$$

For the calculation of the reduction system, some of the elements are set arbitrary based again on the existing grippers. It is the case of the gear wheel and the worm drive. The main parts that define a gear wheel are the primitive diameter (d_p), the number of teeth (z), the modulus (m) and the circular pitch (p) [25].

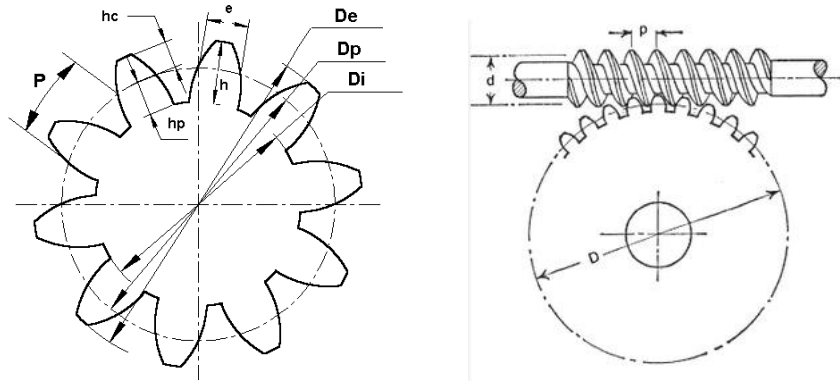


Figure 74. Worm gear variables [26]

For the gear wheel,

$$D_p = 40 \text{ mm and } z_w = 60 \text{ teeth} \quad (Eq. 29)$$

Then,

$$m_w = \frac{D_p}{z} = \frac{2}{3} \cong 0.67 \text{ mm} \quad (Eq. 30)$$

$$p_w = m_w \cdot \pi = 0.67\pi \text{ mm} \quad (Eq. 31)$$

For a gear to work properly, the most important features are the module, the type of gears, the pressure angle and the helix angle.

In this case, our scope will be only to focus on module and pitch study and the other conditions will be assumed. The worm is been decided to have only one tooth, so one

tooth advances for each turn of the gear. Also, the axial pitch of the worm must match the transverse pitch of the wheel, as they work at 90 degrees. Then,

$$p_s = p_w = 0.67\pi \text{ mm} \quad (\text{Eq. 32})$$

Once the closing time and the main parameters are set, the goal is to compute the minimum angular velocity for the motor.

Firstly, it is computed the angular velocity of the gear wheel (ω_w). The closing time is $t_p = 0.5 \text{ s}$ for a circular trajectory of 65° . Note that the lasts 10° to reach the maximum of 75° are excluded because are important for the pinching system.

$$\omega_w = \frac{\varphi_{max}}{t_p} = \frac{65^\circ}{0.67 \text{ s}} = 97.5 \frac{^\circ}{\text{s}} \quad (\text{Eq. 33})$$

And through conversion factors,

$$\omega_w = 97.5 \frac{^\circ}{\text{s}} \cdot \frac{1 \text{ rev}}{360^\circ} \cdot \frac{2\pi \text{ radian}}{1 \text{ rev}} = \frac{13}{24} \pi \text{ rad} \cong 1.7 \frac{\text{rad}}{\text{s}} \quad (\text{Eq. 34})$$

$$\omega_w = 97.5 \frac{^\circ}{\text{s}} \cdot \frac{1 \text{ rev}}{360^\circ} \cdot \frac{60 \text{ s}}{1 \text{ m}} = \frac{65}{4} \text{ rpm} \cong 16.25 \text{ rpm}$$

Now, it is possible to determine the relation of transmission (i) considering that the worm shaft makes one complete revolution per each tooth of the gear wheel and taking into account that the gear wheel has 60 teeth. Then, the gear wheel completes a revolution when the worm shaft has revolutionized 60 times.

$$i = \frac{p}{n} = \frac{1}{60} \quad (\text{Eq. 35})$$

And by definition,

$$i = \frac{\omega_w}{\omega_s} \quad (\text{Eq. 36})$$

$$\omega_s = \frac{\omega_w}{i} = \frac{65}{2} \pi \frac{\text{rad}}{\text{s}} \cong 102.10 \frac{\text{rad}}{\text{s}}$$

$$\omega_s = 975 \text{ rpm}$$

Therefore, a motor of $\omega = 975 \text{ rpm}$ is required.

3.4.3. 3D design

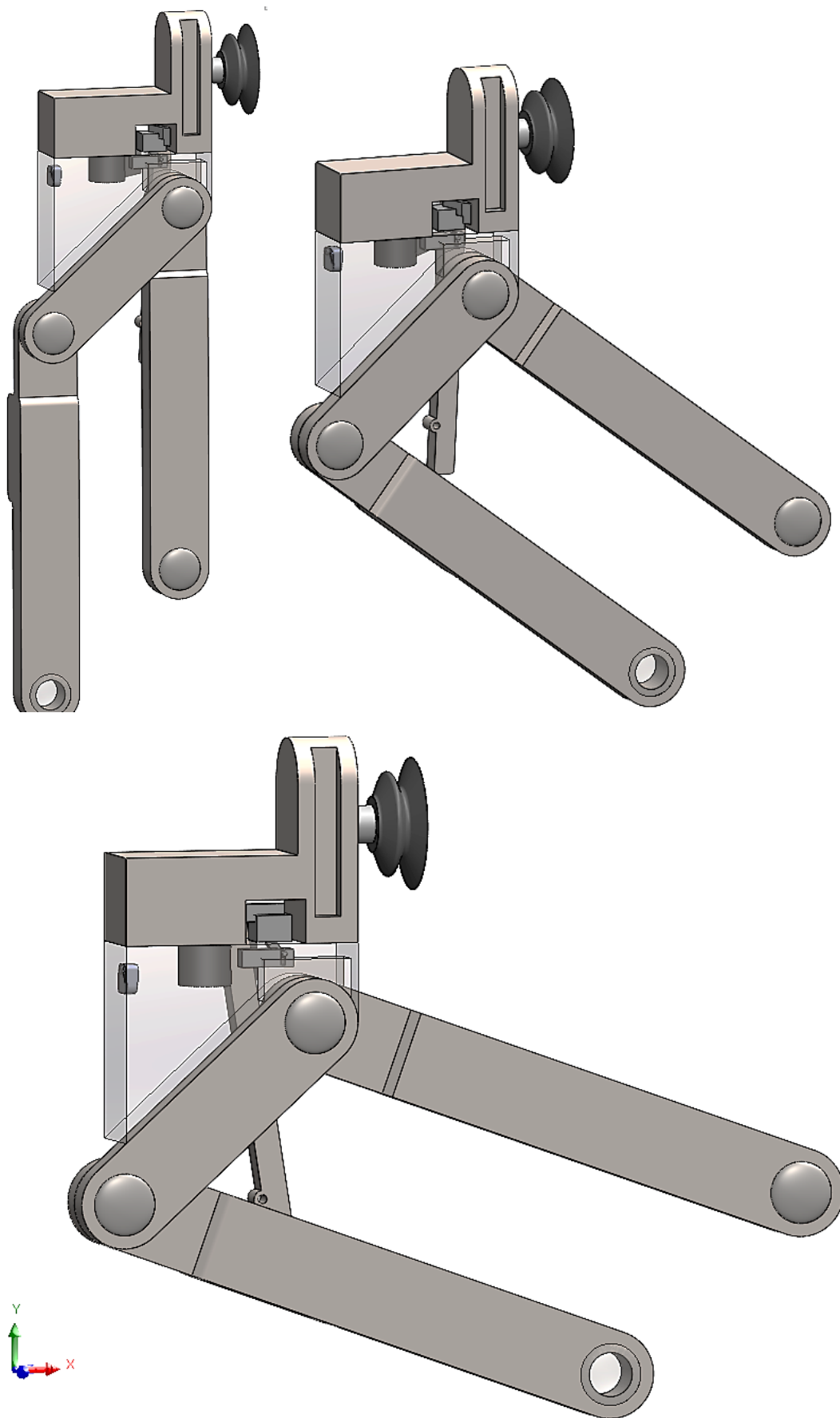
As a part of the process, a 3D prototype of the left finger of the gripper on SolidWorks has been created. Also, all the assembly constraints can be seen in the SolidWorks file on the appendix documentation (“PrototypeAssembly–GRIPPER.sldasm”).

It is important to mention that the 3D includes all the dimensioning of the parts and extra features to make sure the structure has sense. They were not included before because they are not important for the study of the mechanism. However, they have been included in the 3D design to have an understandable 3D that can operate. The main important changes are the following: slots on the support of the fingertip to allocate the locking mechanism and the axis of the wheel, a protuberance on also the support of the fingertip to maintain the L6 at a certain position when the gripper is closed, the increase on the width of the solid L2 to allocate the solid L2S and construction attached to the solid L4 to fixed the axis of L6 revolute joint. Again, their shape is not important nor studied because were not important for the dimensioning of the main structure. This part of the design is considered beyond the scope of the project as it was considered part of the detailed design.

3.5. Results, discussion, and simulation

Mainly speaking, a prototype of the left finger of the gripper has been achieved. In this chapter, the result is showed and discussed.

Let us take a look of the final design.



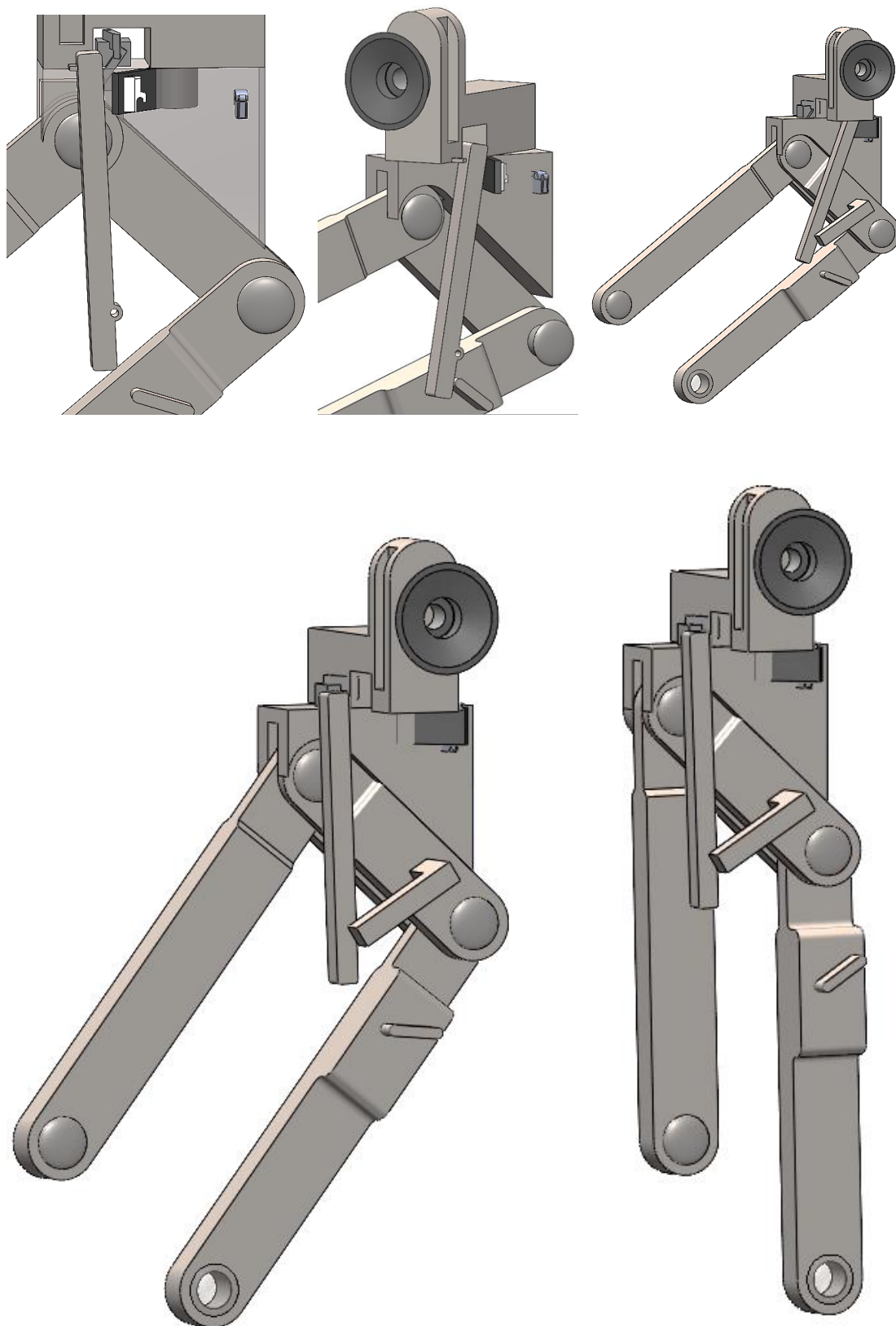


Figure 75. 3D prototype

It is achieved a mechanism that works and allow the user to use either pinching or suction grasping on all the trajectory. The final range of angles are obtained for each grasping type.

Table 9. Parameters of the result

$\varphi_{pinching}$	$\varphi_{suction}$	$\varphi_{switching}$
0 – 65.08°	0 – 65.08°	65.08° – 74.66°

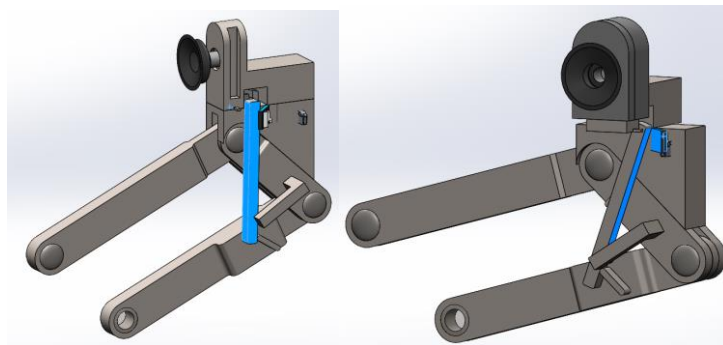


Figure 76. Moments where the angles presented are calculated (initial and final positions for suction switching)

The results match a lot almost exactly with the requirements previously specified where the aim was to reach a range of switching of 65-75°.

Once here, some of the next steps to follow for the continuation of the project are the detailed design, the explanation and industrial drawings of the final assembly, the simulation as well as more analysis such a study of forces and operability, and the construction of the gripper.

However, there are some topics that can produce an error on the real operating of the system that should be discussed before proceeding the project. They are mainly cause of the small dimensions of the gripper. There are some recommendations for a well design that it is been noticed that could not be correctly considered because they are outside the knowledge and scope of this project, especially on the dimensions of holes and thickness of parts. And this could generate problems on the well working of the gripper. A revision of the pieces M1 and L6 should be done before the continuation of the project to fix possible problems of this kind. Also, the small dimension of parts and the operation of complex mechanisms can produce also an inaccurate system that could not operate well on the real life. This also should be considered for further studies on the mechanism and the detailed design.

As a proposal for improvement of the project, maybe a simpler mechanism should be chosen. Although it is possible that some specifications might have to be waived, the result would probably be more competitive on the market and more reliable and aesthetic.

4. Economic, environmental and social assessment

The realization of an economic and environmental implication study is a fundamental task to evaluate the impact of any device or apparatus on the market and on the natural environment. However, in this case, it is not possible to carry out a detailed study of these characteristics due to the lack of detailed design and accurate information about the device.

In situations like this, studies of similar or comparable devices on the market are often used in order to obtain a useful, though not precise, approximation.

As for the cost of the project, this will be divided into two parts. On the one hand, the cost of materials to manufacture a prototype. According to similar projects, the cost of a first prototype creation could be close to 1000€. On the other hand, the cost of the human resources for the design and assembly of the prototype will depend on the hours invested [2].

Regarding the environmental cost of the design and production of a robotic gripper, it can be a complex process and depends on several factors. On the next steps for this gripper, priority will be given to sustainable design (long service life, ease of maintenance and repair), with materials of lower environmental impact (recyclable, light alloys, bioplastics...). Also, energy efficiency (for instance, through renewable energy sources or a good choice on the motor) and waste management during production and operation (collection, recycling and responsible disposal of components and materials at the end of their useful life) will be favored.

Social study and gender equality in the design and construction of a gripper are important aspects to consider to ensure that this process is inclusive and equitable.

In terms of gender equality, gender diversity in the gripper design and construction team is encouraged.

Regarding the social aspect, it will be investigated whether the results of the work can benefit vulnerable groups, such as amputees.

5. Conclusions

The following conclusions arise.

The main objectives are achieved. A gripper that combines the pinching and suction system in one assembly and motor has been created.

Also, a switching system that changes pinching to suction configuration and vice versa without adding a motor.

Firstly, a deep study of the market and the target objects has been performed successfully and be applied on the concrete task specifications of the gripper.

A first mathematical approach on finding a complex unique linkage system is tried but without achieving a feasible solution. However, a final approach based on two different independent mechanism has given a satisfactory solution.

The final mechanism works adequately and is operable on a 3D design environment.

However, some topics could produce an error on the real operating of the system because of the small dimensions and complex mechanisms. Therefore, this should be discussed before proceeding the project. Also, some improvements are recommended.

Finally, it can be concluded that a gripper that combines suction and pinching is possible and is thought to have a lot of room in the market.

6. References

- [1] T. K. Lien, "Gripper technologies for food industry robots," *Woodhead Publishing Limited*, 2013.
- [2] A. C. Luque, "Disseny d'un "gripper" versàtil per robot," Barcelona, 2022.
- [3] OnRobot, "RG2 Gripper Datasheet," [Online]. Available: https://onrobot.com/sites/default/files/documents/Datasheet_RG2_v1.2_EN.pdf.
- [4] F. A. & C. K, "TentacleGripper: Gripping modelled on an octopus tentacle," 2017. [Online]. Available: https://www.festo.com/net/en_group/SupportPortal/Files/630182/Festo_Tentacle_Gripper_en.pdf.
- [5] M. O. K. K. A. S. a. A. O. Hideichi Nakamoto, "A Gripper System for Robustly Picking Various Objects Placed Densely by Suction and Pinching," *IEEE/RSJ International Conference on Intelligent Robots and Systems (IROS)*, 2018.
- [6] K. E. B. D. B. O. B. A. C. K. Nikolaus Correll, "Lessons from the Amazon Picking Challenge," 2007.
- [7] T. G. Company, "MAXXgrip," [Online]. Available: <https://thegrippercompany.com/>.
- [8] R. H. Robotics, "RightPick Gripper," [Online]. Available: <https://righthandrobotics.com/products/rightpick>.
- [9] M. M. M. a. M. H. A. H. Geasa, "Effect of Mechanical Damage on Tomato Fruits under Storage Conditions," *Journal of Soil Sciences and Agricultural Engineering*, 2022.
- [10] I. Russ Engineering Group, "Results of Friction Coefficient Test," 2000. [Online]. Available: <http://www.aspbase.com/assets/files/testing/Coefficient-Test-of-Static-Friction.pdf>.
- [11] M. V. Olga Belova, "Pneumatic Capsule Transport," Research Gate, [Online]. Available: https://www.researchgate.net/publication/306051031_Pneumatic_Capsule_Transport.
- [12] *. J. L. a. G. M. Ehab Hussein Bani-Hani, "Data on the coefficient of static friction between surfaces coated with different sizes of rubber granules produced from used tires," 2019.
- [13] "The Engineering Toolbox," [Online]. Available: https://www.engineeringtoolbox.com/friction-coefficients-d_778.html.
- [14] B. N. J. P. T. V. Tolpekina, "Adhesion and Friction for Three Tire Tread Compounds," *Lubricants*, 2019.
- [15] E. Edge, "Coefficient of Friction Equation and Table Chart," [Online]. Available: https://www.engineersedge.com/coefficients_of_friction.htm.

- [16] G. M. J. K.-H. E. H. M. C. Glenn Elert, "Coefficients of Friction for Rubber," The Physics Factbook, 2005. [Online]. Available: <https://hypertextbook.com/facts/2005/rubber.shtml>.
- [17] KGKRubberPoint, "Friction of Rubber Sliding," 2007. [Online]. Available: https://www.kgk-rubberpoint.de/wp-content/uploads/migrated/paid_content/artikel/652.pdf.
- [18] Z. S. F. M. J. G. X. Y. Sh. Li, "Simulation and Experiment on Conveying Device of Cutting System of Small," *International Journal of Engineering*, 2013.
- [19] A. P. G. Gracia, "Suction Guidelines".
- [20] OnRobot, "DATASHEET - VG10 V1.0 OnRobot," 2023. [Online]. Available: https://onrobot.com/sites/default/files/documents/Datasheet_VG10_v1.0_EN.pdf.
- [21] A. P. Gracia, "Mechanism Design - Computational mechanical design of robotic systems," UPC.
- [22] A. Olsen, "The opercular mouth-opening mechanism of largemouth bass functions as a 3D four-bar linkage with three degrees of freedom," *The Journal of Experimental Biology*, 2017.
- [23] A. P. Gracia, "Kinematics of Robots," Draft January 2012 .
- [24] M. Lubrication, "Worm Gears," [Online]. Available: <https://www.machinerylubrication.com/Read/1080/worm-gears>.
- [25] Engranos, "Los Engranajes," [Online]. Available: <http://engranosexporashidi.blogspot.com/2015/05/>.
- [26] Roymech, "Worm Gears," [Online]. Available: https://www.roymech.co.uk/Useful_Tables/Drive/Worm_Gears.html.
- [27] A. C. Luque, "UPC Commons," [Online]. Available: <https://upcommons.upc.edu/handle/2117/368424>.
- [28] R. PRO, "RS PRO Metric Bronze Worm wheels," [Online]. Available: <https://docs.rs-online.com/f60f/0900766b81580d92.pdf>.
- [29] R. PRO, "Metric Worm Datasheet," [Online]. Available: <https://docs.rs-online.com/fcfa/0900766b81580d94.pdf>.
- [30] R. PRO, "Mellor Electrics Datasheet," [Online]. Available: <https://es.rs-online.com/web/p/motores-dc/2483671>.
- [31] "Matrices y determinantes," [Online]. Available: <https://www.matricesydeterminantes.com/matrices/tipos-de-matrices/matriz-unitaria/>.